



# Amorphous nasal powder advanced performance: in vitro/ex vivo studies and correlation with in vivo pharmacokinetics

Patrícia Henriques<sup>1,2</sup> · Joana Bicker<sup>1,3</sup> · Andreia Carona<sup>1,3</sup> · Margarida Miranda<sup>4,5</sup> · Carla Vitorino<sup>1,4,5</sup> · Slavomíra Doktorovová<sup>2</sup> · Ana Fortuna<sup>1,3</sup> 

Received: 2 June 2023 / Accepted: 16 August 2023 / Published online: 18 September 2023  
© The Author(s) 2023

## Abstract

**Purpose** Amorphous solid dispersions (ASD) for nasal delivery offer the opportunity to increase drug release performance, while using polymers with mucoadhesive properties. The aim of the present study was to apply this solubility enhancement technique to a poorly soluble drug for nasal delivery, while comparing two particle engineering strategies, namely spray dried microparticles and chimeral agglomerates, with the corresponding physical blends with crystalline drug.

**Methods** Formulations of piroxicam were manufactured using varied polymer and particle engineering strategies and evaluated through in vitro drug release and ex vivo permeation studies, as well as nasal deposition and in vivo pharmacokinetic studies.

**Results** ASD with hydroxypropyl methylcellulose (HPMC) showed enhanced drug release and permeation, compared to polyvinylpyrrolidone/vinyl acetate formulations and blends. Nasal deposition of HPMC chimeral agglomerates suggested off-target deposition. In vivo pharmacokinetic studies revealed that spray-dried HPMC-containing microparticles exhibited the highest maximum plasma concentration ( $C_{\max}$ ) and the lowest time to attain it ( $t_{\max}$ ). In vitro release rate and in vivo absorption rate were correlated as well as  $t_{\max}$  and in vitro performance. When excluding the formulation with least nasal targeted deposition, in vitro release and ex vivo permeation performance were also correlated with  $C_{\max}$  and area under the drug concentration-time curve (AUC) from 0 to 1 h, with  $R^2 > 0.89$ .

**Conclusion** ASD for nasal delivery provide fast drug absorption, which depends on the supersaturation ability of the polymer employed. In vitro-in vivo correlations suggested that in vitro release and ex vivo permeation studies are predictive tools regarding nasal absorption.

**Keywords** Nasal powder · Amorphous solid dispersions · Particle engineering · In vitro-in vivo correlations · Nasal deposition

✉ Ana Fortuna  
afortuna@ff.uc.pt; anafortuna@gmail.com

- <sup>1</sup> Laboratory of Pharmacology, Faculty of Pharmacy, Pólo das Ciências da Saúde, University of Coimbra, Azinhaga de Santa Comba, Coimbra 3000-548, Portugal
- <sup>2</sup> R&D, Drug Product Development, Hovione FarmaCiencia SA, Lisbon, Portugal
- <sup>3</sup> Coimbra Institute for Biomedical Imaging and Translational Research (CIBIT), Institute of Nuclear Sciences Applied to Health (ICNAS), University of Coimbra, Coimbra, Portugal
- <sup>4</sup> Coimbra Chemistry Center, Institute of Molecular Sciences (IMS), Department of Chemistry, University of Coimbra, Coimbra, Portugal
- <sup>5</sup> Egas Moniz Center for Interdisciplinary Research (CiiEM), Egas Moniz School of Health & Science, Caparica, Almada, Portugal

## Introduction

Nasal powder delivery has emerged as a promising approach for systemic delivery of both small and large molecules given the large surface area and high permeability of nasal mucosa, leading to fast drug absorption (Fortuna et al. 2014). The majority of nasal products are liquid formulations. However, they present challenges regarding chemical and microbiological stability and fast clearance from the nasal cavity. Powders for nasal delivery provide higher mucoadhesion and stability (Trenkel and Scherließ 2021) and enable the administration of poorly soluble drugs (Tiozzo Fasiolo et al. 2019; Henriques et al. 2022).

In the past decade, there has been a notable rise in the number of poorly soluble drugs both in development and

on the market (Bennett-Lenane et al. 2020; Nunes et al. 2022). Production of amorphous solid dispersions (ASD) is an established formulation strategy to overcome solubility challenges (Williams et al. 2013; Newman 2015). It can be additionally applied to nasal delivery (Pozzoli et al. 2017; Suwabe et al. 2023) with mucoadhesive polymers, increasing both dissolution and residence time of the formulation in the nasal cavity. Common strategies to manufacture ASD for nasal delivery include spray drying to obtain particles within the target size range of 10 to 45  $\mu\text{m}$  (Tiozzo Fasiolo et al. 2018), or smaller particles of 1.5 to 29  $\mu\text{m}$ , further agglomerated into larger agglomerates of 106 to 1000  $\mu\text{m}$  (Colombo et al. 2005). These have been described as chimeral agglomerates since their size is transient and reduces during insufflation (Colombo et al. 2005). The technology of chimeral agglomerates has been shown to improve nasal drug release due to the small size of the primary particles incorporated in a free-flowing powder (Russo et al. 2004; Balducci et al. 2013). In spite of the current knowledge on formulation, manufacturing and characterization of nasal powders (Tiozzo Fasiolo et al. 2018; Henriques et al. 2022), scarce studies compare particle engineering strategies and evaluate the potential of ASD (Pozzoli et al. 2017; Tiozzo Fasiolo et al. 2021; Suwabe et al. 2023). Additionally, predictive *in vitro* methodologies are not standardized (Wadell et al. 2003; Jug et al. 2018; Furubayashi et al. 2020; Gieszinger et al. 2021) and many different apparatus and method variables are used for nasal powder drug release (Huh et al. 2010; Dalpiaz et al. 2015; Colombo et al. 2016; Papakyriakopoulou et al. 2021), permeation (Wadell et al. 2003; Tas et al. 2009; Gonçalves et al. 2016) and deposition (Kundoor and Dalby 2011; Trows and Scherließ 2016; Cunha et al. 2022; D'Angelo et al. 2023). *In vitro-in vivo* correlations (IVIVC) would be a valuable tool to support the use of predictive *in vitro* methodologies as well as to guide formulation and process development (Shen and Burgess 2015; Gieszinger et al. 2021).

In this context, piroxicam (PXC), a non-steroidal anti-inflammatory drug (NSAID) with analgesic properties, was herein chosen as a model low solubility drug for systemic nasal drug delivery. Other NSAIDs have been used for nasal delivery, such as meloxicam (Bartos et al. 2015) and flurbiprofen (Tiozzo Fasiolo et al. 2019) in pre-clinical studies and ketorolac as a commercial nasal spray (Food and Drug Administration 1989). The low solubility of NSAIDs for nasal delivery, namely meloxicam and flurbiprofen, has been addressed in the literature, either through the use of excipients, or as a salt form (Bartos et al. 2015; Horváth et al. 2016; Tiozzo Fasiolo et al. 2019). To our best knowledge, the low solubility of PXC has never been addressed in order to improve drug release and nasal absorption of powder formulations. Studies with other drugs have shown

an enhanced biopharmaceutical performance of amorphous nasal powders compared to crystalline drug material (Gavini et al. 2006, 2011; Jug and Bećirević-Laćan 2008; Elmowafy et al. 2014; Pozzoli et al. 2017; Suwabe et al. 2023). However, these are often compared only with the corresponding blends or crystalline drug, and do not comprise other particle engineering strategies such as chimeral agglomerates.

The purpose of the present work was to understand the relevance of ASD formulations for nasal delivery through *in vitro/ex vivo* performance and *in vivo* pharmacokinetic studies of ASDs of PXC, while investigating the impact of different polymers and comparing two different particle engineering strategies – (i) spray-dried microparticles (SDM) within the nasal size range and (ii) chimeral agglomerates – with the corresponding physical blends as reference. For that, six formulations were developed and evaluated regarding their physicochemical properties and performance through *in vitro* drug release and *ex vivo* permeation. Nasal deposition using human idealized geometry and *in vivo* pharmacokinetic studies with a rat model were then conducted with the selected formulations. Performance methodologies were chosen based on their frequent use in the literature and biomimetic potential (similar conditions to the nasal cavity) (Wadell et al. 2003; Jug et al. 2018; Jurišić Dukovski et al. 2019; Chen et al. 2022; Trenkel and Scherließ 2023). The second aim of this study was to establish IVIVCs of the results obtained, in order to investigate the potential of the methodologies used as predictive tools for nasal powder development.

## Materials and methods

### Materials

PXC was purchased from abcr GmbH (Karlsruhe, Germany). Hydroxypropyl methylcellulose (HPMC) (grade E3, substitution type 2910) was provided by Dow Europe (Horgen, Switzerland) and polyvinylpyrrolidone/vinyl acetate (PVP/VA) by Ashland Specialties (Beveren, Belgium). Water from Milli-Q® Water Purification System (Millipore®, MA, USA) was used and other solvents as acetonitrile, methanol (Merck KGaA, Darmstadt, Germany) and dimethyl sulfoxide (DMSO) (Fisher Scientific, Loughborough, UK) were from analytical or high-performance liquid chromatography (HPLC) grade. Unless otherwise specified, all remaining chemicals were obtained from Sigma-Aldrich (St. Louis, MO, USA).

## Manufacturing and physicochemical characterization of powder formulations

PXC formulations (20%, w/w) were manufactured in a previous work (Henriques et al. 2021). Briefly, 3 different particle engineering strategies were employed, containing either HPMC or PVP/VA, in a total of 6 formulations. SDM, primary particles for agglomeration and polymer microparticles for physical blends were produced by spray drying, using either a lab scale spray-dryer or a commercial scale spray-dryers, after dissolving the materials in a DCM:MeOH 80:20 (w/w) mixture. The process parameters are described in Table 1. The spray-dried formulations were further dried to remove any residual solvents in a vacuum drying oven at 40 °C.

Chimeral agglomerates were produced by vibrating 5 g of the primary particles in a sieve shaker (Haver & Boecker, Oelde, Germany) equipped with two sieves (mesh sizes of 106 and 710 µm) with an amplitude of 2.5 mm for 2 steps of 15 min (total of 30 min). Agglomerates retained on top of the 106 µm sieve were collected.

Physical blends were prepared by mixing polymer microparticles obtained by spray drying with PXC raw material, in a Turbula T2F blender (Willy A Bachofen AG, Muttenz, Switzerland) at 32 rpm for 10 min.

The formulations surface morphology was investigated by scanning electron microscopy (SEM). For that, samples were attached to carbon tapes (Ted Pella Inc., CA, USA) which were fixed in aluminum stubs. Any powder excess was removed by vacuum. Particle morphology was examined by a Phenom ProX scanning electron microscope (Thermo Fisher Scientific, USA) in high vacuum mode and acceleration voltage at 10 kV.

Particle size distribution (PSD) was assessed by laser diffraction in a Sympatec dry dispersion unit (Sympatec HELOS/BR Rodos/M Aspiros Sympatec GmbH, Clausthal-Zellerfeld, Germany). Depending on the formulation, lenses with different measuring ranges were used: R2 (0.45–87.5 µm) and R4 (1.8–350 µm). In the dispersing method, the feed velocity was set to 18 mm/s and the considered

pressure was 1 bar. Measurements were performed in duplicate.

XRPD was performed in an Empyrean® II diffractometer (Malvern Panalytical, Malvern, UK) using a PIXcel1D detector with a copper radiation source, a voltage of 45 kV, and a filament emission of 40 mA. The samples were measured over a 2θ interval of 5–40° with a step size of 0.0131° and time per step of 99.45 s.

## In vitro drug release and ex vivo permeation studies

In vitro drug release and ex vivo permeation studies were performed using vertical Franz diffusion cells (PermeGear, Inc., PA, USA) with a diffusion area of 0.636 cm<sup>2</sup>, with either a dialysis cellulose membrane (MWCO ~ 14,000, average flat width 33 mm, D9652, Sigma-Aldrich) as artificial membrane or porcine nasal mucosa as barrier, respectively.

The fresh mucosa was provided by a local slaughterhouse (Incarpo, Condeixa, Portugal). On the day of experiment, nasal tissue was carefully harvested from the ventral nasal turbinates of the pig and immersed in saline solution (0.9% w/v NaCl in MilliQ Water). Afterwards, it was cut to appropriate size, washed with PBS pH 7.4 and clamped between the donor and receptor compartments of vertical Franz diffusion cells (PermeGear, Inc., PA, USA), with the apical side facing up. Before experiments, the donor chamber was filled with simulated nasal fluid (SNF) (8.77 mg/mL NaCl, 2.98 mg/mL KCl, 0.78 mg/mL CaCl<sub>2</sub>·2H<sub>2</sub>O, pH=6) and leakage to the empty receptor chamber was monitored, in order to assess membrane integrity and proper arrangement on the cell surface (Karavasili et al. 2016).

The receptor compartment comprised 5 mL of SNF, stirred at 600 rpm and maintained at 37 °C ± 0.5 °C (assuring 32 °C at the membrane surface) by a thermostatic water pump, mimicking nasal mucosa physiological conditions. Powder formulations (5 mg) were applied directly to the donor compartment followed by the addition of 50 µL of SNF in order to promote powder wetting. Samples from the receptor compartment (400 µL) were collected at 0.17 (10 min), 0.33 (20 min), 0.5 (30 min), 1, 1.5, 2, 3, 4, 6 and

**Table 1** Spray-drying process parameters

| Formulation                         | Spray-dryer                                                                      | C <sub>solids</sub> (% w/w) | F <sub>feed</sub> (kg/h) | T <sub>out</sub> (°C) | F <sub>drying</sub> (kg/h) |
|-------------------------------------|----------------------------------------------------------------------------------|-----------------------------|--------------------------|-----------------------|----------------------------|
| SDM                                 | Büchi model B-290 (Flawil, Switzerland) with custom made extended drying chamber | 5                           | 1.5                      | 60                    | 20                         |
| Primary particles for agglomeration | Büchi model B-290                                                                | 5                           | 1.5                      | 30                    | 20                         |
| Polymers for physical blends        | PVP/VA PSD4 (Gea, Düsseldorf, Germany)                                           | 10                          | 152                      | 60                    | 1500                       |
|                                     | HPMC Mobile Minor (Gea, Düsseldorf, Germany)                                     | 5                           | 4                        | 50                    | 75                         |

C<sub>solids</sub> – Solids concentration; F<sub>atom</sub> – atomization gas flow rate for two-fluid nozzle; F<sub>drying</sub> – drying gas flow rate; F<sub>feed</sub> – liquid feed flow rate; HPMC – hydroxypropyl methylcellulose; NA – not applicable; P<sub>feed</sub> – pressure for pressure nozzle; PVP/VA - polyvinylpyrrolidone/vinyl acetate; SDM - spray-dried microparticles; T<sub>out</sub> – outlet drying temperature

8 h. After each collection, the same volume was replaced with pre heated SNF. Collected samples were centrifuged for 5 min at 12,100 g (MiniSpin, Eppendorf Ibérica S.L., Madrid, Spain) before HPLC analysis.

The samples were analyzed by HPLC diode array detector in an integrated chromatograph model LC-2040 C-3D (Shimadzu Corporation, Tokyo, Japan) (Table 2). The coefficient of variation (CV, %) and deviation from nominal value (Bias, %) were in accordance with the international bioanalytical guidelines issued by the International Council for Harmonization of Technical Requirements for Pharmaceuticals for Human Use (International Council For Harmonization of Technical Requirements for Pharmaceuticals for Human Use 2022) (Table 2).

Artificial membrane inertness was assessed by incubating the dialysis cellulose membrane in SNF with a PXC known concentration at  $32 \pm 1$  °C for 24 h. The membrane was considered to be inert if at least a 95% PXC recovery was attained.

Experiments were carried out in triplicate for in vitro drug release studies and triplicate in 3 independent experiments for ex vivo permeation studies.

The attained cumulative drug release curves were fitted to different mathematical models in order to identify the possible mechanisms involved in drug release and obtain parameters for IVIVC, specifically zero order, first order, Higuchi and Korsmeyer-Peppas (Bruschi 2015).

## Nasal deposition studies

Powders (20 mg) were manually filled in the same devices used for in vivo studies. Nasal deposition was evaluated using the Alberta Idealized Nasal Inlet (AINI) (Copley

**Table 2** Chromatographic conditions and partial validation parameters obtained for the high performance liquid chromatography (HPLC) assays applied for the quantification of piroxicam in in vitro drug release and ex vivo permeation studies

|                                                     |                                                                       |
|-----------------------------------------------------|-----------------------------------------------------------------------|
| Mobile Phase                                        | Water:Acetonitrile 55:45 (v/v) and 0.1% (v/v) of trifluoroacetic acid |
| Column                                              | InfinityLab Poroshell 120 EC-C18 (150 mm x 4.6 mm; 2.7 μm) at 45°C    |
| Flow rate (mL/min)                                  | 1.0                                                                   |
| Detection Wavelength (nm)                           | 337                                                                   |
| Injection Volume (μL)                               | 10                                                                    |
| Retention Time (min)                                | 3.0                                                                   |
| Calibration Range (μg/mL)                           | 0.03 to 50                                                            |
| Coefficient of determination ( $R^2$ ) <sup>a</sup> | 0.9999                                                                |
| LLOQ (μg/mL)                                        | 0.03                                                                  |
| Precision (% CV) <sup>a</sup>                       | 3.69 to 11.41                                                         |
| Accuracy (% Bias) <sup>a</sup>                      | -5.96 to 6.06                                                         |

Bias, deviation from nominal value; CV, coefficient of variation; LLOQ, lower limit of quantification; <sup>a</sup> Inter-day values (n=3)

Scientific, Nottingham, United Kingdom) coupled with Next Generation Impactor (NGI) (Copley Scientific, Nottingham, United Kingdom). This idealized nasal airway geometry in aluminum was developed according to computational fluid dynamics simulations performed in a set of realistic nasal geometries, in order to mimic human nasal deposition (Chen et al. 2020, 2022). The drug was quantified in the four regions of interest: vestibule (nostril), the turbinates, the olfactory region and the nasopharynx. To mitigate particle bounce, the AINI and NGI stages were coated with Brij solution (0.15 g/ml Brij in ethanol) in glycerol (1mL Brij solution for 5 g glycerol) (Murphy et al. 2022). The device was actuated at a 45° angle between the inlet plane of the vestibule and the device tip (Chen et al. 2022), with an inhalation flow rate of 15 L/min (Kiaee et al. 2019), in 3 actuations of 2 s each, based on previous experience using this device. Piroxicam quantification was performed by HPLC analysis in the AINI regions, NGI stages and device after washing with fixed volumes of methanol. The mass balance was calculated by the following equation,

$$\text{Mass Balance (\%)} = \frac{m_{\text{recovered}}}{m_{\text{filled}}} \times 100 \quad (1)$$

where  $m_{\text{recovered}}$  is the PXC mass quantified in all AINI regions, NGI stages and device after actuation and  $m_{\text{filled}}$  is the PXC mass filled in the device before actuation. In order to normalize the results, data are presented as the fraction of recovered dose on AINI regions and NGI stages, without considering dose retention in the device or lost in the equipment.

Experiments were carried out in triplicate.

## In vivo studies

### Animals and ethical considerations

Healthy male Wistar rats (RccHan®:WIST) were acquired from Charles River Laboratories (L'Arbresle, France) and housed under controlled environmental conditions (12 h light/dark cycle, temperature  $22 \pm 1$  °C; relative humidity  $50 \pm 5\%$ ) with *ad libitum* access to food (4RF21, Mucedola, Italy) and tap water. Animals were acclimated for at least one week before experiments.

All animal procedures were conducted in agreement with the international regulations of the European Directive (2010/63/EU) regarding the protection of laboratory animals used for scientific purposes and with the Portuguese law on animal welfare (Decree-Law 113/2013). The experimental and care procedures were reviewed and approved by the Animal Welfare Board (ORBEA, 02-2021—Órgão Responsável pelo Bem-Estar Animal) at the Faculty of

Pharmacy of the University of Coimbra and the Portuguese Directorate-General for Food and Veterinary (DGAV). All efforts were made to minimize the number of animals used and their suffering.

### In vivo pharmacokinetic study

Fifteen Wistar Han® rats, weighing between 235 and 315 g, were randomly divided into five groups (3 animals each). Each group was treated with a single dose of one of the following treatments: (a) Intravenous (IV) bolus administration of a 0.27 mg/kg PXC dose through the tail vein; (b) Intranasal (IN) administration of SDM HPMC powder formulation; (c) IN administration of SDM PVP/VA; (d) IN administration of chimeral agglomerates of HPMC and (e) IN administration of PXC blend with HPMC. All IN formulations were administered at a dose of 0.3 mg of PXC.

Each group was treated with a single dose of PXC and blood samples (~0.3 mL) were collected into heparinized tubes at 0.33, 1, 2, 4, 6, 8, 12, 24 and 30 h post-administration. Before PXC administration, rats were anesthetized with ketamine (75 mg/kg, i.p.) and xylazine (10 mg/kg, i.p.), and their lateral tail vein was cannulated by inserting the Introcán® Certo IV indwelling cannula (22G; 0.9 × 2.5 mm; B. Braun, Melsungen, Germany). This procedure allowed the obtainment of a complete plasma concentration-time profile from each rat. After recovery from anesthesia, rats were administered and blood was collected through the inserted cannula. The collected blood volume was periodically replaced by the injection of sterile heparinized saline (5 I.U./mL). Blood samples were immediately centrifuged at 1514 g for 10 min at 4 °C to obtain plasma, which was processed for drug analysis (Gonçalves et al. 2017).

For IV administration, PXC was firstly dissolved in DMSO at 20 mg/mL and then added to a solution of sterile saline and polyethylene glycol 400 50:50 (v/v) to a final concentration of 0.18 mg/mL (0.9% DMSO). Animals received an IV bolus (1.5 ml/kg) into the lateral tail vein opposite to the inserted cannula.

For IN administration, powders (~1.5 mg, corresponding to ~0.3 mg of PXC) were filled in a commercial device adapted for administration to small animals. Before administration, the rat was placed in right lateral decubitus, making the left nostril accessible for powder insufflation. The tip of the nasal insufflator was inserted into the nostril with 1–2 mm depth. The pump was actuated and the powder was emitted in one shot. Immediately after use, the device was re-weighed to determine the quantity of emitted powder and calculate the actual administered dose.

At the final timepoint of 30 h, animals were sacrificed by decapitation under deep isoflurane anesthesia. At this timepoint, brain and lungs were excised, gently washed

with sodium chloride 0.9% solution, dried with a sterile compress and weighed. Using a THOMAS® Teflon tissue homogenizer, tissues were homogenized with 3 mL (brain) or 4 mL (lungs) of sterile saline per gram of tissue and tissue homogenates were centrifuged at 4147 g for 15 min at 4 °C (Serralheiro et al. 2014; Gonçalves et al. 2021).

### Drug analysis

The HPLC method to quantify PXC in plasma was firstly developed and validated in human plasma (see supplementary material) and then adapted and partially validated for rat plasma and tissues.

Sample preparation consisted of adding 10 µL of naproxen working solution (internal standard, at 100 µg/mL in acetonitrile) and 50 µL of hydrochloric acid 0.1 M to 100 µL of plasma or lung homogenate supernatant, or 150 µL of brain homogenate supernatant. After vortex-mixing for 5 s, samples were subjected to two liquid-liquid phase extractions with diethyl ether. Briefly, 330 µL of diethyl ether was added and, after vortex-mixing for 1 min, samples were centrifuged for 5 min at 12,100 g (MiniSpin, Eppendorf Ibérica S.L., Madrid, Spain). The organic phase was collected into a glass tube and the procedure was repeated. Organic phases were totally evaporated at 60 °C under a slight nitrogen stream. The solid residue was reconstituted in 100 µL of mobile phase (water:acetonitrile 55:45% v/v with 0.1% v/v trifluoroacetic acid), followed by 1 min of vortex-mixing and centrifugation for 5 min at 12,100 g (MiniSpin, Eppendorf Ibérica S.L., Madrid, Spain). Supernatant (20 µL) were injected in the HPLC system. Lung samples were additionally filtered through Costar® Spin-X® (0.22 µm, Corning, Inc., NY, USA) at 12,100 g for 3 min before injection of 20 µL.

A Shimadzu HPLC system (Shimadzu Corporation, Kyoto, Japan) equipped with a solvent release model (LC-20 A), a degasser (DGU-20A5), an autosampler (SIL-20AHT), a column oven (CTO-10ASVP) and a diode array detector (SPD-M20A) were used. Control and monitoring of the apparatus, as well as result collection were performed by LCsolution Software (Shimadzu Corporation, Kyoto, Japan). Chromatographic separation was achieved with a Infinity-Lab Poroshell 120 EC-C18 (150 mm × 4.6 mm; 2.7 µm), at 45 °C with isocratic elution using water:acetonitrile 55:55 (v/v) with 0.1% trifluoroacetic acid at 1 mL/min as mobile phase. PXC and internal standard were detected at 337 nm and 262 nm, at retention times of approximately 3.0 and 5.4 min, respectively. To assure elution of all sample impurities, run time was defined as 18 min.

The full validation in human plasma (see supplementary material) and partial validation in rat plasma, brain and lung was performed according to the international guidelines of

bioanalytical method validation of the European Medicines Agency (EMA) (European Medicines Agency 2011) and the Food and Drug Administration (FDA) (Food and Drug Administration 2018), as demonstrated in Table 3.

### Pharmacokinetic analysis

For IN administration, concentrations were dose normalized, since administered doses comprised variability inherent to device actuation. Normalization was accomplished by dividing each concentration by the actual dose administered (0.26 to 0.37 mg) and multiplying by the average theoretical dose of 0.3 mg, according to the following equation:

$$\frac{\text{Plasma concentration normalized } \left(\frac{\mu\text{-g}}{\text{mL}}\right)}{\frac{\text{Observed plasma concentration } \left(\frac{\mu\text{-g}}{\text{mL}}\right)}{\text{Dose administered } (\mu\text{g})} \times \text{Average theoretical dose } (300\mu\text{g})} = \quad (2)$$

The mean normalized experimental concentration ( $n=3$ ) versus time profiles were plotted and submitted to non-compartmental pharmacokinetic analysis, using WinNonlin software, version 5.2 (Pharsight Co, Mountain View, CA, USA). The pharmacokinetic parameters included the area under the drug concentration-time curve (AUC) from time zero to one hour ( $AUC_{1h}$ ), the AUC from time zero to time of the last measurable drug concentration ( $AUC_t$ ) which were calculated by the linear trapezoidal rule; the AUC from time zero to infinity ( $AUC_{inf}$ ) which was calculated by the addition of  $AUC_t$  and the quotient between the last quantifiable concentration and the apparent elimination rate constant. Additionally, the apparent terminal elimination half-life ( $t_{1/2}$ ) and mean residence time (MRT) were also determined. The maximum concentration ( $C_{max}$ ) in plasma and tissues of PXC and the corresponding time to reach  $C_{max}$  ( $t_{max}$ ) were directly obtained from the experimental data. Absolute bioavailability [F (%)] of each formulation was calculated by the following equation:

$$F (\%) = \frac{AUC_{t(IN)} \times Dose_{IV}}{AUC_{t(IV)} \times Dose_{IN}} \times 100 \quad (3)$$

Where  $AUC_{t(IN)}$  is the  $AUC_t$  for IN administration,  $AUC_{t(IV)}$  is the  $AUC_t$  for IV administration,  $Dose_{IV}$  is the IV administered dose and  $Dose_{IN}$  is the IN administered dose.

Additionally, monocompartmental analysis was performed to obtain additional parameters for IVIVC. These pharmacokinetic parameters included  $t_{max}$ , and absorption rate ( $k_a$ ) for IN formulations.

### In vitro/in vivo data correlation (IVIVC)

The data generated in the in vitro release studies, ex vivo permeation, and in vivo pharmacokinetic studies of PXC formulations were used to develop the IVIVC. Two levels of correlation, B and C, were investigated according to EMA guidelines (European Medicines Agency 2014).

In order to establish level B IVIVC, in vitro release rate was compared with the in vivo absorption rate. For level C IVIVC, the in vitro release and ex vivo permeation parameters considered were: (i) percentage of drug released at 0.33 h (20 min) (ii) percentage of drug permeated at 0.33 h (20 min) (iii) percentage of drug released at 1 h (iv) percentage of drug permeated at 1 h. These parameters were correlated with pharmacokinetic parameters including  $C_{max}$ ,  $t_{max}$ ,  $AUC_{1?h}$  obtained with non-compartmental analysis and  $t_{max}$  obtained with monocompartmental analysis ( $t_{max}$ MCA). For both IVIVC levels, linear regression analysis was applied using least squares method to estimate the regression parameters, where the correlation coefficient ( $R^2$ ) was evaluated. Additionally, non-linear regression (four-parameter logistic regression and exponential plateau regression) was applied to level B IVIVC as alternative curve fits.

**Table 3** Validation parameters of the HPLC method employed for the quantification of piroxicam in rat plasma, brain and lung

|                                        | Rat plasma         | Rat brain          | Rat lung           |
|----------------------------------------|--------------------|--------------------|--------------------|
| Calibration range ( $\mu\text{g/mL}$ ) | 0.08–24            | 0.027–10           | 0.5–100            |
| Regression equation <sup>a</sup>       | $y=0.2014x+0.0006$ | $y=0.3308x+0.0006$ | $y=0.2575x-0.0133$ |
| Coefficient of determination ( $R^2$ ) | 0.9951             | 0.9957             | 0.9970             |
| LLOQ ( $\mu\text{g/mL}$ )              | 0.08               | 0.027              | 0.5                |
| Precision <sup>b</sup> (% CV)          | 1.43 to 6.89       | 2.96 to 11.13      | 5.96 to 12.55      |
| Accuracy <sup>b</sup> (% Bias)         | -10.73 to -6.44    | -13.24 to 11.38    | 0.01 to 5.66       |

Bias, deviation from nominal value; CV, coefficient of variation; LLOQ, lower limit of quantification;

<sup>a</sup> Equation of the calibration curve is given by the general equation of  $y=mx+b$ , with  $m$  corresponding to the slope and  $b$  to the intercept. The equation represents the peak area signals of PXC to that of the internal standard ( $y$ ), versus the corresponding concentration of PXC ( $x$ ), with a weighted linear regression using  $1/x^2$  as the best weighting factor. <sup>b</sup>Inter-day values ( $n=3$ )

## Statistical analysis

Data were processed using GraphPad Prism 8 (GraphPad Software, San Diego, USA). In vitro data are expressed as mean  $\pm$  standard deviation (SD), and in vivo pharmacokinetic profiles are expressed as mean  $\pm$  standard error of the mean. Two-way analysis of variance (ANOVA) with Tukey multiple comparison test were used when appropriate. Differences were considered statistically significant when  $p < 0.05$ .

## Results and discussion

### Manufacturing and physicochemical characterization of powder formulations

Nasal powders can be manufactured by spray drying, an established technology that allows the control of particle size and shape, as well as the generation of ASD, a strategy to improve solubility of drugs. For this study, the mucoadhesive polymers HPMC and PVP/VA were selected as the amorphous stabilizers in ASD of the model drug, poorly soluble piroxicam. These polymers were selected due to their common use in spray dried dispersions (Vig and Morgen 2017), as well as polymers in mucosal delivery (Salamat-Miller et al. 2005; Ugwoke et al. 2005; Sosnik et al. 2014). It is worth noting that HPMC (substitution type 2910) is one of the few excipients in the FDA inactive ingredients database, as it has been used in FDA-approved nasal powders (Food and Drug Administration 2023). This further reinforces its relevance for nasal powder formulations.

Spray drying can additionally be applied to fine tune particle properties and manufacture SDM within the target nasal size range of 10 to 45  $\mu\text{m}$ . Alternatively, spray drying can produce smaller primary particles that are subsequently agglomerated into chimeral agglomerates. Despite the extra manufacturing step, this strategy has the advantage of possible faster dissolution of the smaller primary particles. Here, these two manufacturing strategies were applied to the model drug poorly soluble PXC and benchmarked against

the respective physical blends with crystalline drug, all at 20% drug load.

Table 4 shows the physicochemical characterization of powder formulations regarding PSD and solid state. SDM containing PVP/VA or HPMC showed a  $Dv_{50}$  of 28.4 and 44.6  $\mu\text{m}$  respectively, which falls within the nasal size range of 10 to 45  $\mu\text{m}$  (Tiozzo Fasiolo et al. 2018). Primary particles for agglomeration were produced by spray drying PSD within the desired range for agglomeration (Colombo et al. 2005) ( $Dv_{50}$  between 2 and 3  $\mu\text{m}$ ). Chimeral agglomerates were then obtained by vibrating microparticles in sieves with the intended size range. The respective physical blends were produced as a control at the same drug load by mixing polymer microparticles with PXC raw material. Amorphous PXC without excipients as an additional control sample could not be obtained, as this drug is not a good glass former (Van Eerdenbrugh et al. 2010) and rapidly crystallizes without a stabilizer excipient.

SEM micrographs of powder formulations are shown in Fig. 1. PVP/VA based microparticles showed a smooth round surface, while HPMC microparticles revealed a wrinkled morphology, both for SDM and primary particles for agglomeration (Fig. 1a–b and e–f). The particle structures obtained by spray drying are closely linked to the physicochemical properties of the materials being dried, including solute viscoelastic properties and molecular size (de Souza Lima et al. 2020). The ability of HPMC polymer to induce wrinkled morphology has been previously reported (Jüptner and Scherließ 2020).

Physical blends were obtained by mixing polymer microparticles obtained by spray drying with PXC raw material. Given that PXC raw powder contained a high percentage of particles below 10  $\mu\text{m}$ , a larger polymer microparticle carrier was added to minimize the powder fraction with potential of reaching the lungs. The  $Dv_{50}$  of the blends was within the nasal size range (Table 4). SEM micrographs showed small needle-like structures alone or distributed on the polymer microparticles surface, which correspond to PXC raw material (Fig. 1c–d).

XRPD analysis was carried out to determine solid state characteristics. Diffractograms of SDM and agglomerates

**Table 4** Physicochemical characterization of powder formulations

| Analysis                 |             | Spray-dried microparticles |                  |                  | Primary particles for Chimeral agglomerates |                 | Blends                      |                             |
|--------------------------|-------------|----------------------------|------------------|------------------|---------------------------------------------|-----------------|-----------------------------|-----------------------------|
|                          |             | Unit                       | PVP/VA           | HPMC             | PVP/VA                                      | HPMC            | PVP/VA                      | HPMC                        |
| <b>Particle size</b>     | <b>Dv10</b> | $\mu\text{m}$              | $13.10 \pm 0.39$ | $17.43 \pm 0.47$ | $0.50 \pm 0.01$                             | $0.61 \pm 0.01$ | $2.98 \pm 0.02$             | $3.95 \pm 0.03$             |
|                          | <b>Dv50</b> | $\mu\text{m}$              | $28.40 \pm 0.62$ | $44.60 \pm 0.33$ | $2.01 \pm 0.03$                             | $2.86 \pm 0.12$ | $20.72 \pm 0.05$            | $16.42 \pm 0.05$            |
|                          | <b>Dv90</b> | $\mu\text{m}$              | $50.31 \pm 0.61$ | $82.92 \pm 0.29$ | $4.97 \pm 0.03$                             | $6.74 \pm 0.41$ | $47.29 \pm 0.73$            | $33.66 \pm 0.13$            |
| <b>Solid form (XRPD)</b> |             | -                          | Amorphous        | Amorphous        | Amorphous                                   | Amorphous       | Has PXC crystalline content | Has PXC crystalline content |

HPMC - hydroxypropyl methylcellulose; NA, not applicable; PVP/VA - polyvinylpyrrolidone/vinyl acetate; PXC – piroxicam; XRPD – X-ray powder diffraction

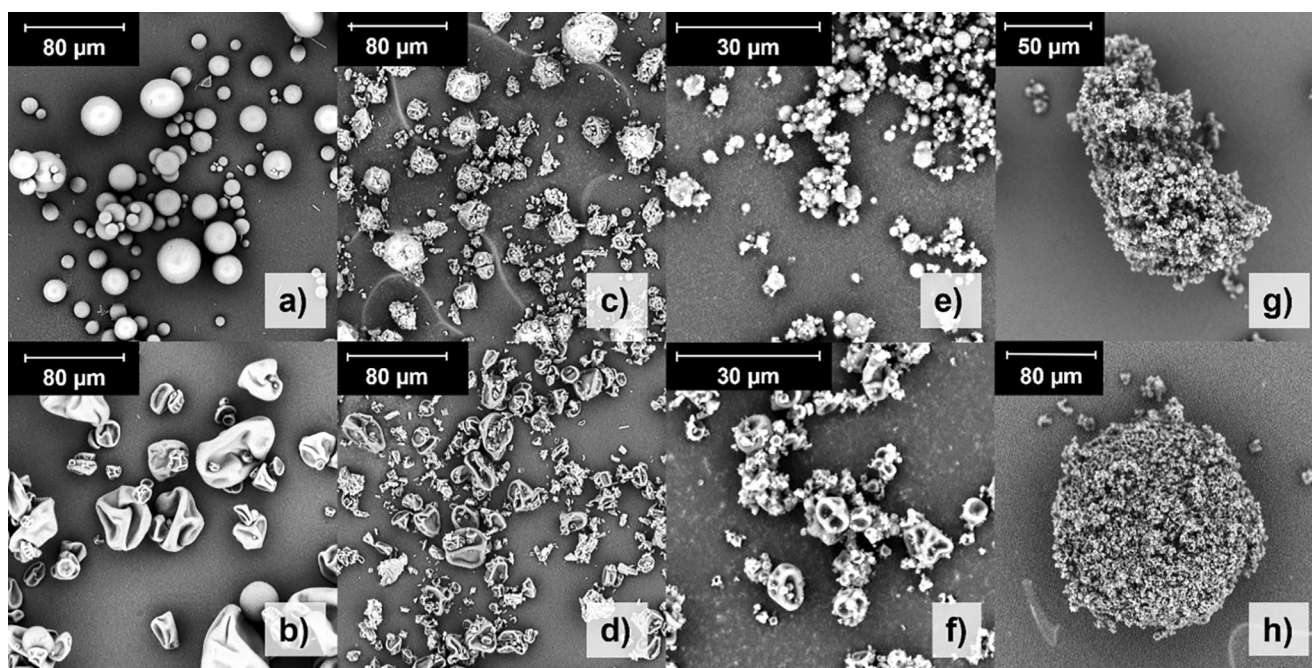


**Fig. 1** SEM micrographs of spray-dried microparticles [a] PVP/VA, b) HPMC], physical blends [c] PVP/VA; d) HPMC], primary particles for agglomeration [e] PVP/VA; f) HPMC] and chimeral agglomerates [g] PVP/VA; h) HPMC], 1000x magnification for a-d, 2000x magnifi-

cation for e-f, 1400x magnification for g), 900x magnification for h). HPMC - hydroxypropyl methylcellulose; PVP/VA - polyvinylpyrrolidone/vinyl acetate; SEM - scanning electron microscopy

formulations showed no crystalline peaks characteristic of PXC (supplementary material, Fig. S1). It is noteworthy that the HPMC-based SDM formulation showed a peak in XRPD diffractogram at  $\sim 32^\circ$ , which is consistent with the HPMC raw material behavior and not with the PXC diffractogram (supplementary material, Fig. S1B). As the blends were manufactured by mixing crystalline drug with amorphous polymer, the resulting formulation showed a diffractogram with the amorphous pattern of the polymer and the crystalline peaks characteristic of the drug.

### In vitro drug release studies

Franz diffusion cells were used to study the drug release profile of the powder formulations having one of two different polymers (PVP/VA and HPMC), manufactured by three different strategies (SDM, chimeral agglomerates and blends). Membrane inertness was confirmed, since a 98.5% PXC recovery was attained.

This methodology makes it possible to mimic physiological conditions of the nasal cavity, including temperature, medium and slow powder hydration in a humid environment similar to that encountered in the nasal cavity (Jug et al. 2018). The drug transport across the artificial membrane is governed by the drug concentration in the donor compartment, resulting from the dissolution of the solid formulations. In vitro drug release studies were conducted over 8 h.

Even though powders can remain in the nasal cavity for up to several hours (Marttin et al. 1998), this time frame may exceed the residence time of formulations in the nasal cavity, due to the mucociliary clearance.

The percentage of PXC released was plotted as a function of time (Fig. 2). Due to the low solubility of PXC ( $53 \pm 1 \mu\text{g/mL}$  as experimentally determined in the SNF pH=6 at  $37^\circ\text{C}$ ) and the reduced receptor compartment volume, sink conditions could not be met at the last two sampling points for SDM of HPMC and at the last timepoint for chimeral agglomerates of HPMC (concentrations from 17.7 to  $22.6 \mu\text{g/mL}$ ). In general, low percentages of PXC were released throughout the test (up to 15.1% w/w). This is associated with the very low diffusion area and low fluid volume on the donor compartment for the quantity of powder considered. In fact, comparing with in vivo human conditions, the available area for drug transport in Franz diffusion cells is approximately 236 times lower than the nasal cavity surface ( $0.636 \text{ cm}^2$  vs.  $150 \text{ cm}^2$  (Mygind and Dahl 1998)), and the quantity of powder is only around 10 times lower than the maximum recommended for nasal administration (Tiozzo Fasiolo et al. 2018) ( $5 \text{ mg}$  vs.  $50 \text{ mg}$  (Tiozzo Fasiolo et al. 2018)). Therefore, a higher drug release percentage would be expected under closer in vivo conditions.

The results evidence that both the manufacturing strategy and the polymer have impact on the release behavior of the powder formulations. All SDM and chimeral agglomerates

had higher percentages of drug released than the corresponding blends during the first 3 h, with 2.8–10.0% of drug release for SDM and chimeral agglomerates and 2.1–2.5% for blends at 3 h. For HPMC formulations, this was valid for the 8 h of the test. Additionally, it could be expected that chimeral agglomerates would have a higher drug release than SDM, given the considerably smaller size of the primary particles that would promote faster drug release. Surprisingly, that was only the case for PVP/VA-based formulations (Fig. 2). This is possibly due to the dominating effects of the fast drug dissolution of the amorphous powder formulations with generation of supersaturated solutions, hindering the effect of changes in particle size.

Regarding the polymer, SDM and chimeral agglomerates formulations containing HPMC showed higher mean percentages of drug release. From the 20-minute timepoint onwards, SDM of HPMC exhibited a significantly ( $p < 0.001$ ) higher percentage of drug release, when compared to all other formulations. Blend formulation presented a slower release, with major differences seen in the first 2 h (Fig. 2), most likely due to the crystalline state of the drug. The amorphous form of the drug in the polymer matrix can generate a supersaturated solution, increasing the drug dissolved which is available to cross the artificial membrane. The polymer has a major impact on the ability of an ASD to achieve and maintain supersaturation (Vig and Morgen 2017). Indeed, HPMC may sustain the supersaturated drug for a longer period of time, allowing a higher drug release. Even though PVP/VA may promote some degree of supersaturation, this polymer may lead to a faster drug precipitation, thereby decreasing the release rate.

The in vitro drug release profiles were evaluated using different kinetic models – zero order, first order, Higuchi and Korsmeyer-Peppas model – for the timepoints in sink conditions. According to the coefficients of determination ( $R^2$ ), adjusted  $R^2$  and root mean square deviation, the SDM and chimeral agglomerates release was best characterized by the Korsmeyer-Peppas model (Table 5). This mathematical

model ( $k_{KP} \cdot t^n$ ) has been widely used to characterize drug release kinetics from polymer systems. The diffusion exponent ( $n$ ) is an indicator of the drug release mechanism, where four scenarios can be possible: (i)  $n$  approximately 0.5 — Fickian diffusion process, (ii)  $n = 1$  — non-Fickian diffusion process (zero-order model), (iii)  $0.5 < n < 1.0$  — non-Fickian or anomalous transport and (iv)  $n > 1$  — super case II transport (Bruschi 2015; Simões et al. 2020). As shown in Table 6, the values of  $n$  for SDM and chimeral agglomerates were closer to 0.5, indicating that these formulations followed the Fickian drug transport mechanism where diffusion is the dominant mechanism for drug release. Diffusion is characterized by fast solvent diffusion to the inner matrix and slow polymeric relaxation (Bruschi 2015). Our findings are in accordance with reported studies where the drug release of nasal spray-dried formulations containing a polymer was also characterized by a diffusion-controlled mechanism (Hasçiçek et al. 2003; Elmowafy et al. 2014). The corresponding blends were better characterized by the first-order kinetic model of drug release, where the release rate is concentration dependent. As expected, the different best fit models suggest that the drug arrangement within the polymer – either molecularly dispersed into an amorphous solid dispersion, or physically mixed (crystalline drug) – is a determinant for the drug release kinetics. Nevertheless, since the Korsmeyer-Peppas model provided good correlation coefficients for all formulations ( $R^2 > 0.995$ ), its release rate coefficient ( $k_{KP}$ ) was used for further IVIVC (Table 6).

Aiming at a fast absorption of PXC after nasal powder administration, formulations should guarantee a prompt dissolution and diffusion across the mucosa (Tiozzo Fasiolo et al. 2019). SDM and chimeral agglomerates formulations of HPMC showed the most promising results.

## Ex vivo permeation studies

Porcine nasal mucosa has been widely used in nasal drug permeation models (Wadell et al. 2003; Fransén et al. 2007;

**Fig. 2** In vitro cumulative drug release profile of powder formulations. Results report to the mean  $\pm$  standard deviation calculated from 3 replicates. CA – chimeral agglomerates; HPMC – hydroxypropyl methylcellulose; PVP/VA – polyvinylpyrrolidone/vinyl acetate; SDM – spray-dried microparticles

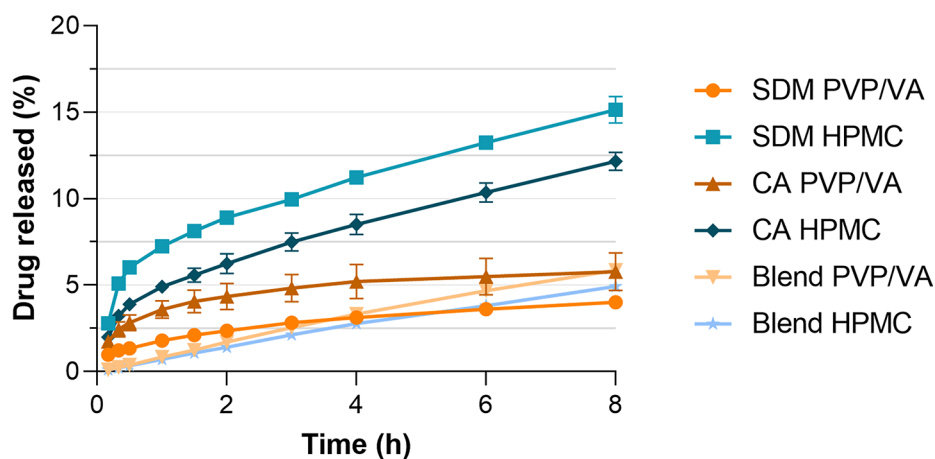


**Table 5** Coefficient of determination ( $R^2$ ), adjusted  $R^2$  and root mean square deviation (RMSD) resulting from the application of the kinetic mathematical models zero order, first order, Higuchi and Korsmeyer–Peppas.

|              | Zero order |                |        | First order                      |                |         | Higuchi             |                |        | Korsmeyer–Peppas   |                |         |
|--------------|------------|----------------|--------|----------------------------------|----------------|---------|---------------------|----------------|--------|--------------------|----------------|---------|
|              | $k_0, t$   |                |        | $F_{max} \cdot (1 - e^{-k_1 t})$ |                |         | $k_H \cdot t^{0.5}$ |                |        | $k_{KP} \cdot t^n$ |                |         |
|              | $R^2$      | Adjusted $R^2$ | RMSD   | $R^2$                            | Adjusted $R^2$ | RMSD    | $R^2$               | Adjusted $R^2$ | RMSD   | $R^2$              | Adjusted $R^2$ | RMSD    |
| SDM PVP/VA   | 0.3830     | 0.3830         | 0.9513 | 0.9228                           | 0.9142         | 0.3365  | 0.9584              | 0.9584         | 0.2470 | 0.9992             | 0.9991         | 0.03431 |
| SDM HPMC     | 0.2902     | 0.2902         | 3.001  | 0.9517                           | 0.9448         | 0.7829  | 0.9173              | 0.9173         | 1.024  | 0.9851             | 0.9830         | 0.4345  |
| CA PVP/VA    | -0.3022    | -0.3022        | 2.025  | 0.9406                           | 0.9340         | 0.4325  | 0.7530              | 0.7530         | 0.8819 | 0.9863             | 0.9848         | 0.2075  |
| CA HPMC      | 0.5240     | 0.5240         | 2.145  | 0.9232                           | 0.9136         | 0.8617  | 0.9804              | 0.9804         | 0.4354 | 0.9962             | 0.9958         | 0.1906  |
| Blend PVP/VA | 0.9936     | 0.9936         | 0.1586 | 0.9994                           | 0.9994         | 0.04712 | 0.8729              | 0.8729         | 0.7059 | 0.9980             | 0.9978         | 0.08852 |
| Blend HPMC   | 0.9939     | 0.9939         | 0.1282 | 0.9996                           | 0.9996         | 0.03266 | 0.8758              | 0.8758         | 0.5785 | 0.9987             | 0.9986         | 0.05876 |

CA – chimeral agglomerates; HPMC – hydroxypropyl methylcellulose; PVP/VA – polyvinylpyrrolidone/vinyl acetate; RMSD – root mean square deviation; SDM – spray-dried microparticles

**Table 6** Regression coefficients obtained from the application of the kinetic mathematical model Korsmeyer–Peppas. Data are expressed as mean  $\pm$  standard error of the mean

|              | Korsmeyer–Peppas - $k_{KP} \cdot t^n$ |                 |        |
|--------------|---------------------------------------|-----------------|--------|
|              | $k_{KP}$                              | $n$             | $R^2$  |
| SDM PVP/VA   | 1.82 $\pm$ 0.01                       | 0.38 $\pm$ 0.01 | 0.9992 |
| SDM HPMC     | 6.99 $\pm$ 0.18                       | 0.34 $\pm$ 0.03 | 0.9851 |
| CA PVP/VA    | 3.45 $\pm$ 0.08                       | 0.27 $\pm$ 0.02 | 0.9863 |
| CA HPMC      | 4.80 $\pm$ 0.08                       | 0.42 $\pm$ 0.01 | 0.9962 |
| Blend PVP/VA | 0.91 $\pm$ 0.03                       | 0.90 $\pm$ 0.02 | 0.9980 |
| Blend HPMC   | 0.77 $\pm$ 0.02                       | 0.90 $\pm$ 0.02 | 0.9987 |

CA – chimeral agglomerates; HPMC - hydroxypropyl methylcellulose; PVP/VA - polyvinylpyrrolidone/vinyl acetate; SDM – spray-dried microparticles

Vitorino et al. 2020), since it resembles the human nasal histology and physiology (Wadell et al. 1999) thereby providing a successful and biorelevant model for nasal absorption studies (Fransén et al. 2007). In this study, the transport of PXC across porcine nasal mucosa was evaluated in Franz-type diffusion cells, using the same conditions of in vitro release experiments.

Figure 3 depicts the ex vivo permeation profiles of PXC formulations across porcine nasal mucosa. Similar to in vitro drug release studies, sink conditions could not be met at all timepoints, namely for SDM and chimeral agglomerates of HPMC at the last three sampling points and both blends at the last two timepoints. Additionally, the steady-state flux could not be calculated as the drug concentration in donor compartment is not constant, depending on kinetic processes such as supersaturation and precipitation (Nunes et al. 2023), and some formulations do not present a linear relationship in the cumulative permeation curve even when considering initial timepoints up to 1 h.

The results showed higher drug permeation for SDM and chimeral agglomerates of HPMC throughout the entire duration of the experiment. SDM and chimeral agglomerates of PVP/VA presented higher permeation than PXC blends in the first 30 min (Fig. 3). However, from the 1 h and 2 h timepoints, PXC blends presented greater average permeation than SDM and chimeral agglomerates of PVP/VA respectively, with statistically significant differences between both blends and SDM of PVP/VA from the 3 h timepoint onward ( $p < 0.001$ ) and between blends and chimeral agglomerates of PVP/VA from the 4 h timepoint onward ( $p < 0.01$ ).

SDM and corresponding chimeral agglomerates exhibited very similar permeation profiles with no statistically significant differences except between SDM and chimeral agglomerates of HPMC at 1 and 1.5 h. However, within these particle engineering strategies, different polymers showed high impact on drug permeation. As mentioned before, for these amorphous formulations, HPMC may sustain a supersaturated drug solution in the donor compartment for longer

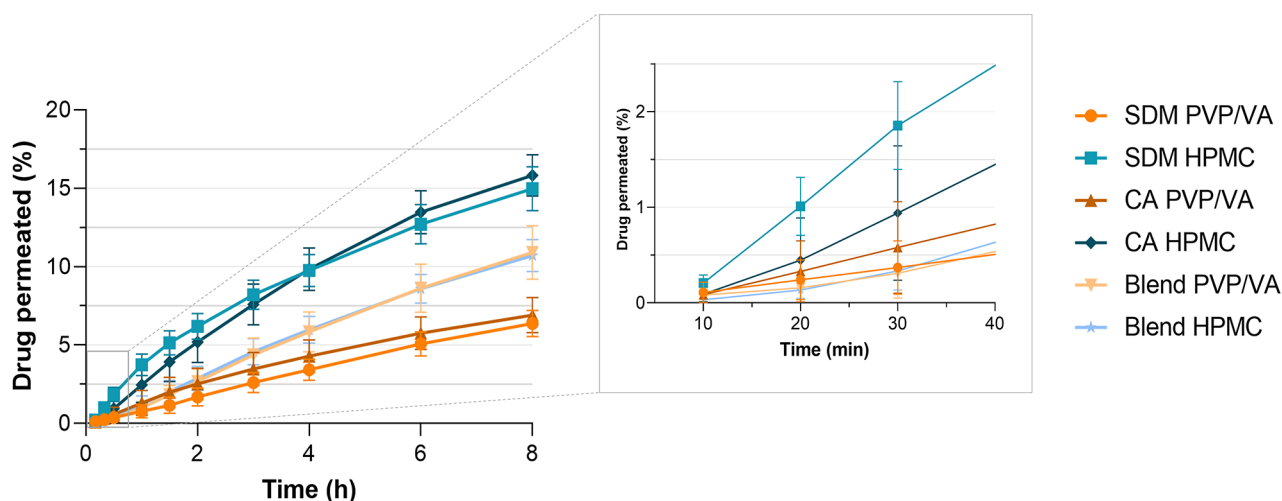


**Fig. 3** Ex vivo cumulative permeation of powder formulations for 8 h (left) and the first 40 min (right). Results are expressed as mean  $\pm$  standard deviation. CA – chimeral agglomerates; HPMC - hydroxypropyl

methylcellulose; PVP/VA - polyvinylpyrrolidone/vinyl acetate; SDM – spray-dried microparticles

time, leading to a higher quantity of dissolved drug available to permeate the mucosa (Tiozzo Fasiolo et al. 2019). SDM and chimeral agglomerates of PVP/VA may also generate supersaturated solutions but for a shorter period of time, leading to higher permeation than the corresponding blend with crystalline drug for the first 30 min. The polymer did not affect the permeation of physical blends, which have similar profiles, indicating that HPMC and PVP/VA only affect permeation through solubility enhancement.

The PXC formulations do not comprise permeability modifiers. Additionally, this drug has high nasal permeability (Henriques et al. 2023), having a lipophilic character ( $\log P = 3.06$ ) (Szabó-Révész 2018) and belonging to Class II of the Biopharmaceutical Classification System of drugs (high permeability through the gastro-intestinal membranes) (Amidon et al. 1995; Mirza et al. 2010). Therefore, the diffusion rate through porcine mucosa should be primarily dependent on the drug release profile of the formulation (Henriques et al. 2022), with correlations between ex vivo permeation and in vitro release profiles. In fact, the first 1.5 h of permeation testing showed very similar results to in vitro release testing in terms of formulation ranking. However, in permeation studies, the blends showed a superior performance than amorphous formulations of PVP/VA from earlier timepoints. This tendency was observed in the in vitro release studies, in which the drug released from SDM and chimeral agglomerates of PVP/VA reached a plateau, in contrast to the blends. The artificial dialysis cellulose membrane and porcine nasal mucosa are different barriers, with the latter being thicker and more complex. Thus, drug transport across nasal mucosa is expected to occur more slowly (Tiozzo Fasiolo et al. 2019). As anticipated, PXC concentrations on the receptor compartment in ex vivo permeability

studies were lower than in in vitro release studies during the first hour for all formulations. This can explain the lower performance of amorphous PVP/VA formulations in permeation studies, since permeation is slow during the short period of time where supersaturation occurs before drug precipitation. These results suggest that ASD for nasal delivery should be able to maintain the supersaturated state and prevent drug precipitation in supersaturated solutions, in order to improve drug release and permeation of a crystalline drug.

Based on the in vitro/ex vivo results, four formulations were selected for nasal deposition studies and in vivo evaluation, namely the formulations of HPMC and SDM of PVP/VA. SDM and chimeral agglomerates of HPMC were selected due to higher drug release and permeation, and the corresponding blend was selected as a comparator. Additionally, SDM of PVP/VA was also tested to study the impact of a different polymer and to establish IVIVC of formulations with different release rates, as recommended by EMA and FDA guidelines (Food and Drug Administration 1997; European Medicines Agency 2014).

### Nasal deposition studies

The selected formulations for in vivo studies were submitted to nasal deposition studies using an idealized nasal airway geometry that mimics human nasal deposition, the AINI (Chen et al. 2020, 2022). This model makes it possible to estimate the quantitative deposition in different parts of the nasal cavity. It was coupled with NGI to provide a detailed deposition profile of the entire respiratory tract. Particles with deposition outside the AINI (NGI stages) were considered to have more potential to reach the gastrointestinal

tract and the lungs. Tests were conducted at 15 L/min flow, as reported in the literature as a representative flow rate in nasal deposition studies (Pozzoli et al. 2017; Jüptner et al. 2019; Kiaee et al. 2019; Gomes dos Reis et al. 2020). Additionally, the NGI can be operated at this flow rate without a pre-separator, with known aerodynamic diameter cut sizes for each stage (between 0.98 and 14.1  $\mu\text{m}$   $d_{50}$  aerodynamic diameter) (Marple et al. 2004). An actuation angle of 45° was also chosen based on nasal deposition studies, including nasal powders (Kundoor and Dalby 2011; Jüptner et al. 2019; Chen et al. 2020).

Figure 4 shows the fraction of recovered dose on AINI regions and NGI stages for each tested formulation. Deposition on the olfactory region and turbinates did not show statistically significant differences between formulations. In the vestibule, only SDM of PVP/VA and blend of HPMC showed statistically significant differences in deposition fraction ( $p=0.04$ ). Chimeral agglomerates of HPMC had lower deposition on nasopharynx and higher deposition on NGI stages, comparing to all the other formulations with statistically significant differences (Fig. 4). The mass balance was higher than 77% for all formulations (supplementary material, Table S4). The United States Pharmacopeia indicates a mass balance acceptance criterion of 85–115% in cascade impaction tests of dry powder inhalers (US Pharmacopeia 2021). However, the unsealed AINI system due to the rigid vestibule inlet along with the manual actuation of the device promotes powder losses that could justify this value.

Powder physical properties, such as particle size and morphology, affect particle impaction and therefore the aerodynamic profile (Jüptner et al. 2019; Farinha et al. 2022). However, no differences were observed in deposition on the turbinates and olfactory region for the different formulations tested. This suggests that deposition on these areas is robust to changes in these formulations' physical properties, considering the range of PSD tested, the device

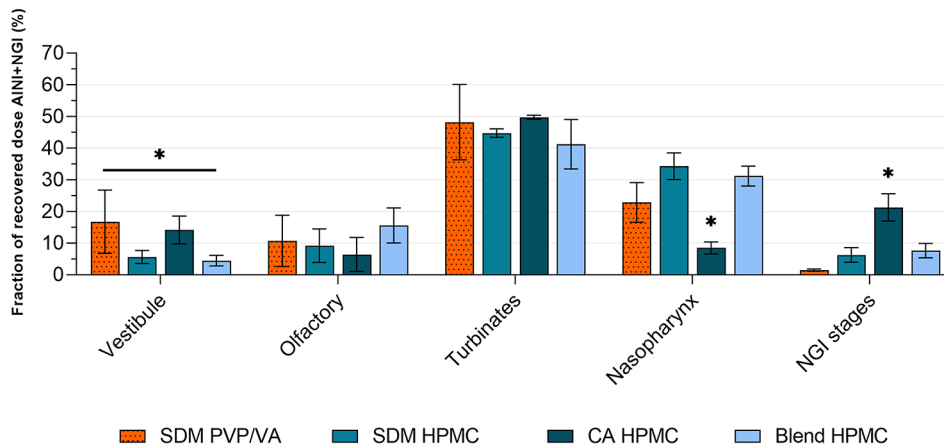
and the method variables used. The airstream rate, limited by the selected device (Henriques et al. 2022), may have a more determinant role on deposition profile on these areas.

Deposition on the nasopharynx and NGI stages was different for the chimeral agglomerates. The size of agglomerates is transient, with a reduction during insufflation that depends on interparticle cohesion and agglomerate mechanical resistance (Russo et al. 2004). In the case of HPMC chimeral agglomerates, the generated fragments showed higher potential to reach the gastrointestinal tract and the lungs than the other formulations, given the significantly higher deposition on the NGI stages. In fact, on average, 21.3% of this formulation deposited on NGI stages, while for the other formulations it was below 7.7%. Additionally, HPMC agglomerates had, on average, 4.11% deposition on NGI stages 5 and 6 ( $1.36 < d_{50} < 3.3 \mu\text{m}$ ), while other formulations had below 0.62% average deposition. This fraction of the formulation can deposit on small airways and alveoli region, since particles are within the aerodynamic size range of 1 to 5  $\mu\text{m}$  (Buttini et al. 2012). The results suggest that deposition of HPMC agglomerates is less nasal targeted with more off-target drug losses.

### In vivo piroxicam plasma concentrations and pharmacokinetic analysis

The selected four formulations were administered into the nose of rats in order to study the PXC pharmacokinetic profile and the impact of different particle engineering strategies and excipients in ASD. The animal model was chosen based on literature studies using the rat for nasal powder administration (Dalpiaz et al. 2008; Gavini et al. 2011; Cho et al. 2015; Rasso et al. 2015, 2018; Tiozzo Fasiolo et al. 2021), and the possibility of collecting sequential plasma samples (Gonçalves et al. 2017), complying with the reduction in 3Rs principle – Replacement, Reduction and Refinement.

**Fig. 4** Fraction of recovered dose on AINI regions and NGI stages of PXC formulations. Results are expressed as mean  $\pm$  standard deviation. \*denotes  $p < 0.05$  as statistically significant. CA – chimeral agglomerates; HPMC – hydroxypropyl methylcellulose; PVP/VA – polyvinylpyrrolidone/vinyl acetate; SDM – spray-dried microparticles



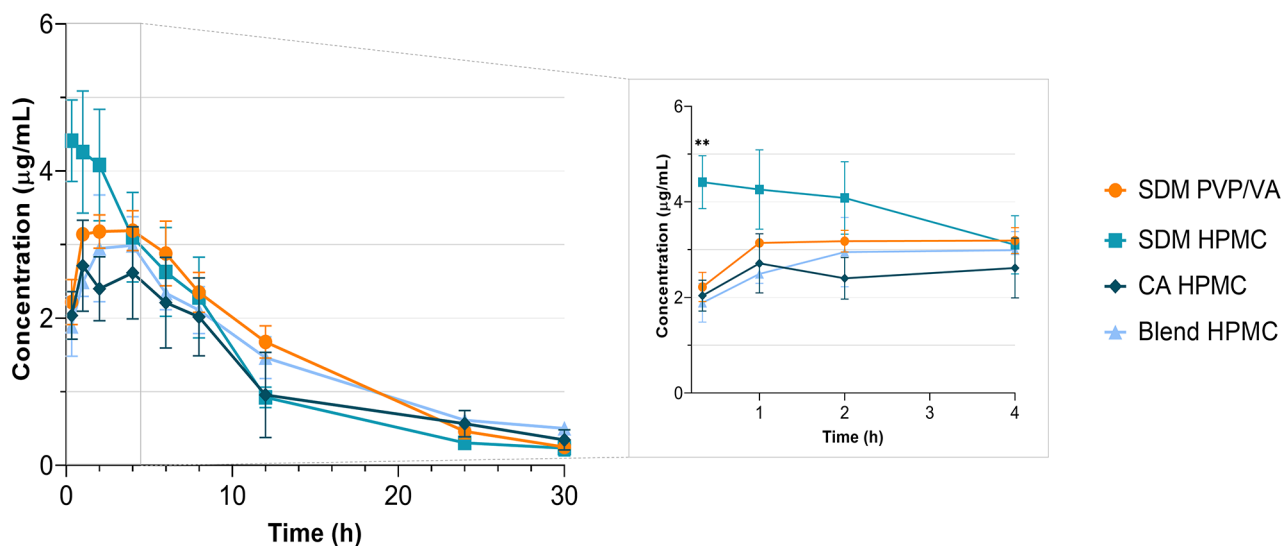


**Fig. 5** Plasma concentration-time profiles of piroxicam for the complete duration of the in vivo pharmacokinetics experiments (left) and the first 4 h (right) after intranasal administration of powder formulations. \*\* $p < 0.01$  was considered as statistically significant. CA

**Table 7** Pharmacokinetic parameters following intranasal or intravenous administration of piroxicam by non-compartmental analysis

| Pharmacokinetic parameters         | SDM PVPVA <sup>a</sup> | SDM HPMC <sup>a</sup> | CA HPMC <sup>a</sup> | Blend HPMC <sup>a</sup> | IV <sup>b</sup> |
|------------------------------------|------------------------|-----------------------|----------------------|-------------------------|-----------------|
| $T_{max}$ (h)                      | 2.33                   | 0.89                  | 2.33                 | 3.33                    | 0.33            |
| $C_{max}$ ( $\mu\text{g/mL}$ )     | 3.35                   | 4.68                  | 2.76                 | 3.26                    | 13.11           |
| $AUC_{1h}$ ( $\mu\text{g h/mL}$ )  | 2.16                   | 3.63                  | 1.93                 | 1.78                    | 11.81           |
| $AUC_t$ ( $\mu\text{g h/mL}$ )     | 46.05                  | 41.06                 | 36.41                | 44.70                   | 40.41           |
| $AUC_{inf}$ ( $\mu\text{g h/mL}$ ) | 48.46                  | 43.28                 | 41.36                | 53.12                   | 44.71           |
| $t_{1/2}$ (h)                      | 6.42                   | 6.24                  | 9.68                 | 11.72                   |                 |
| MRT (h)                            | 10.32                  | 8.92                  | 13.55                | 16.06                   | 9.68            |
| F (%) <sup>c</sup>                 | 29.98                  | 26.73                 | 23.70                | 29.10                   | -               |

<sup>a</sup> Parameters estimated considering a normalized PXC dose of 0.3 mg

<sup>b</sup> Parameters estimated considering a PXC dose of 1.5 ml/kg of 0.18 mg/mL PXC solution (0.0780 to 0.0799 mg of PXC)

<sup>c</sup> Absolute intranasal bioavailability (F) was calculated based on  $AUC_t$  values

$AUC_{1h}$ , Area under the concentration time-curve from time zero to 1 h;  $AUC_{inf}$ , Area under the concentration time-curve from time zero to infinite;  $AUC_t$ , Area under the concentration time-curve from time zero to the last quantifiable drug concentration; CA – chimeral agglomerates;  $C_{max}$ , Maximum peak concentration; F, absolute intranasal bioavailability; HPMC - hydroxypropyl methylcellulose; MRT, Mean residence time; PVP/VA - polyvinylpyrrolidone/vinyl acetate; SDM – spray-dried microparticles;  $t_{1/2}$ , Apparent terminal elimination half-life;  $t_{max}$ , Time to achieve the maximum peak concentration

The average normalized concentration–time profiles of PXC in plasma after nasal powder administration is presented in Fig. 5. The main pharmacokinetic parameters of each individual concentration–time profile estimated by non-compartmental analysis are summarized in Table 7, as well as absolute bioavailability of each formulation.

– chimeral agglomerates; HPMC - hydroxypropyl methylcellulose; PVP/VA - polyvinylpyrrolidone/vinyl acetate; SDM – spray-dried microparticles

After nasal powder administration, the  $C_{max}$  of PXC was attained in plasma between 0.33 and 4 h, ranging from 1.53 to 5.60  $\mu\text{g/mL}$ . SDM of HPMC presented the highest  $C_{max}$  and lowest  $t_{max}$ , suggesting a faster absorption of PXC. For this formulation, PXC plasma concentration at 20 min was significantly higher ( $p < 0.01$ ) than the other formulations. This indicates that this formulation could provide a faster onset of action with quicker and effective therapeutic action, as desired for pain relief. However, this formulation also presented the lowest  $t_{1/2}$  and MRT, leading to lower systemic exposure for the duration of the experiment (41.06  $\mu\text{g h/mL}$ ). SDM of PVP/VA and chimeral agglomerates of HPMC had a similar  $t_{max}$ , followed by the blend with HPMC with the highest  $t_{max}$ . In general, amorphous formulations provided lower  $t_{max}$ , indicating that the faster drug release provided by these formulations has, as expected, impact on drug absorption. SDM of PVP/VA provided the second higher  $C_{max}$ , followed by blend of HPMC and chimeral agglomerates of HPMC. The pharmacokinetic profiles obtained for SDM of PVP/VA and blend of HPMC were comparable, with close  $C_{max}$  and bioavailability values (Table 7). Even though SDM of PVP/VA provided lower  $t_{max}$  and higher systemic exposure in the first hour, faster elimination (lower  $t_{1/2}$ ) led to similar bioavailability compared to the blend formulation. This is in accordance with the in vitro results, where drug release from SDM of PVP/VA was superior in early timepoints but reached a plateau, while the blend of HPMC presented a continuous drug release. The same tendency was observed in permeation studies where

the blend of HPMC provided higher drug permeation only from the 30-minute timepoint onward.

Surprisingly, chimeral agglomerates of HPMC provided the lowest  $C_{\max}$  and  $AUC_t$ . Indeed, drug release and permeation studies suggested a similar profile with SDM of HPMC (Figs. 2 and 3). Additionally, plasma concentration–time profile showed two peaks (Fig. 5), which was not characteristic in the other formulations. This suggests that this formulation could have a less targeted deposition profile leading to partial drug deglutition or lung delivery with a later absorption. Even though there are anatomical differences between the rat and human nose (Henriques et al. 2022), nasal deposition studies in a human idealized nasal airway geometry corroborated these findings, where chimeral agglomerates of HPMC showed a less targeted nasal deposition with 21.3% deposition on NGI stages (Fig. 4). In fact, PXC oral absorption in humans provides a  $t_{\max}$  (4.78 to 5.22 h (Rasetti-Escargueil and Grangé 2005) similar to values observed for the second peak.

At the final timepoint of 30 h, PXC was quantified in the brain and lungs of each animal, to detect possible accumulation of the drug in these tissues. The obtained concentrations were below the LLOQ for all animals. In fact, at this timepoint, the drug had been vastly eliminated with low plasma concentrations of 0.08 to 0.67  $\mu\text{g/mL}$ . For the most promising formulation, full pharmacokinetic studies in tissues should be performed to evaluate drug accumulation at earlier timepoints and relate with or predict possible adverse effects.

### In vitro-in vivo correlations

IVIVC is a mathematical model able to predict in vivo response of drug products based on in vitro properties, which normally include the rate or extent of drug dissolution or release (Shen and Burgess 2015). These relationships are normally categorized in different levels, including level A of a point-to-point correlation between in vitro and in vivo profiles, level B of a one-point relationship that can be between in vitro dissolution rate constant and absorption rate and level C of a one-point relationship between quantity dissolved/released at a specific time and one mean pharmacokinetic parameter as  $C_{\max}$ ,  $t_{\max}$  or AUC (European Medicines Agency 2014). Here, we attempted to establish level B and C correlations for PXC nasal formulations, based on in vitro release and permeation results and in vivo rat pharmacokinetics profile. It should be noted that the in vitro/ex vivo values used for IVIVC were obtained in sink conditions, assuring that the amount of drug dissolved in the receptor would not affect the drug release and permeation rate, reflecting the in vivo environment. For poorly soluble drugs, it can be particularly challenging to obtain

sink conditions with aqueous media (Phillips et al. 2012). In the present work, sink conditions could not be met at the last 2 or 3 timepoints for in vitro release and ex vivo permeation studies respectively. Strategies to overcome this challenge include the use of surfactants or organic solvents on the aqueous media or increasing the volume of the medium (Phillips et al. 2012). However, surfactants and organic solvents can damage the ex vivo membrane (Bao et al. 2018), and the static Franz diffusion cell does not allow volume change. Therefore, SNF was the selected biorelevant medium for ex vivo permeation studies, and the same medium was applied in in vitro drug release studies. Despite employing an aqueous medium and a poorly soluble drug, all the values selected for IVIVC, including the percentage of drug release or permeation at 0.33 and 1 h and the drug release rate (Korsmeyer–Peppas model), were obtained in sink conditions.

Level B correlations can include either a relationship between in vitro dissolution/release time and in vivo residence time or in vitro dissolution/release rate constant and absorption rate (European Medicines Agency 2014). However, since drug release was not complete in our studies, the in vitro release rate constant obtained by the Korsmeyer–Peppas model was correlated with an absorption rate obtained by monocompartmental analysis (Fig. 6a). Linear regression provided a  $R^2$  of 0.725. Visual inspection of the plot suggests a better fit with non-linear correlation models where a plateau occurs at higher absorption rates, for example with an exponential plateau equation. A maximum drug release rate value for increasing absorption rates, as suggested by the plateau, would limit the application of the correlation model to formulations with release rates below the maximum value. However, additional points would be necessary to confirm this hypothesis.

For level C correlations, percentage of drug release or permeation at 0.33 and 1 h were correlated with the pharmacokinetic parameters  $C_{\max}$ ,  $t_{\max}$ ,  $AUC_{1h}$  (non-compartmental analysis) and  $t_{\max}$ MCA (monocompartmental analysis). Early in vitro and in vivo timepoints were selected since we observed a fast nasal absorption for powder formulations, with the shortest  $t_{\max}$  of 0.89 h, and an impact of supersaturation on earlier timepoints in in vitro experiments. Additionally,  $AUC_t$  or  $AUC_{\text{inf}}$  data were not considered in IVIVC since they showed different formulation rankings than in vitro experiments.

The  $t_{\max}$ MCA parameter was included after conducting a monocompartmental analysis (Table 8). Formulations presented little differentiation in  $t_{\max}$  with non-compartmental analysis due to limited blood collections at early timepoints, an inherent limitation of sequential collection. Therefore, normalized concentration–time profiles were fitted to a monocompartmental model which has been previously used

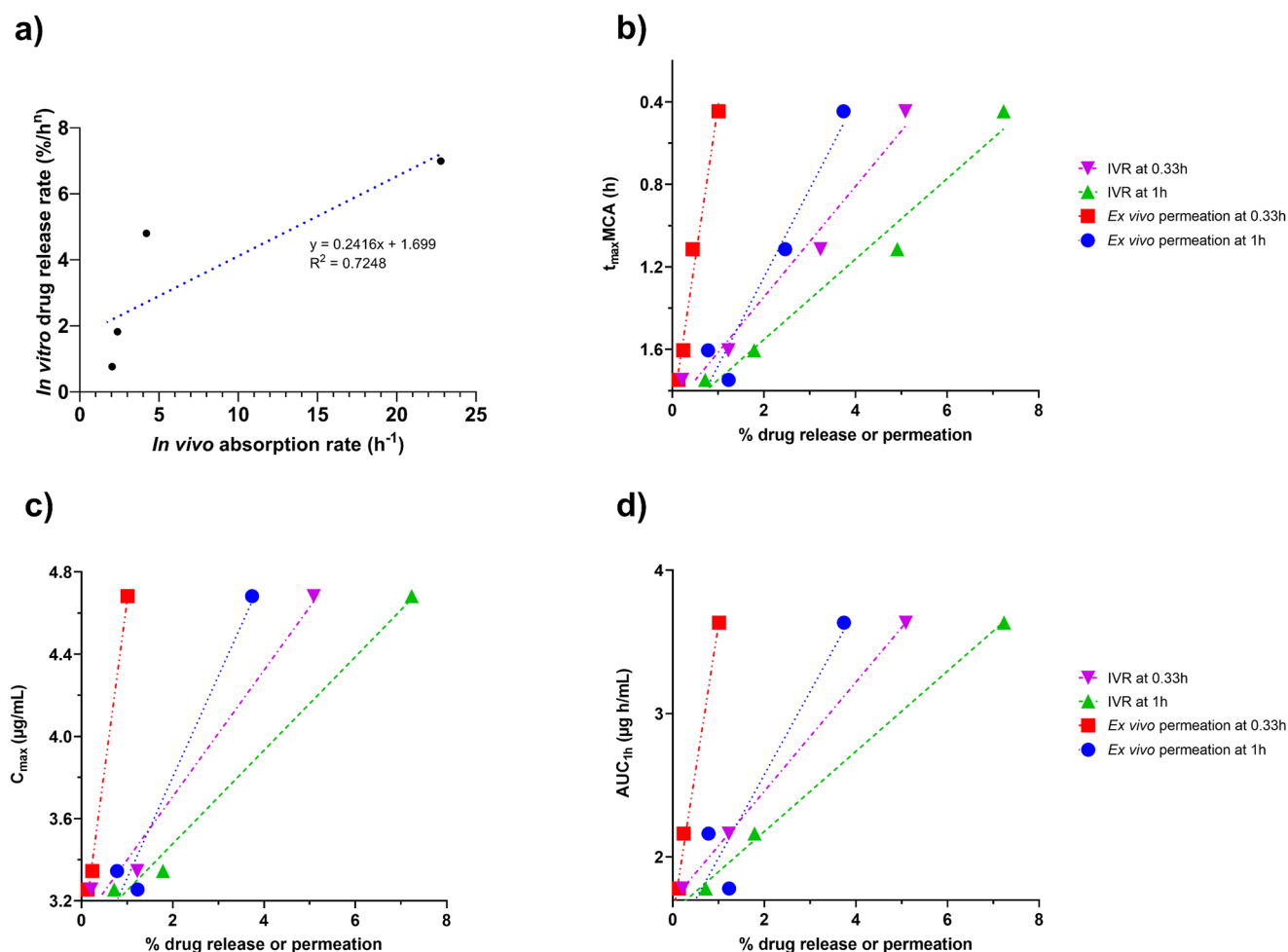


**Fig. 6** In vitro-in vivo correlations between (a) Korsmeyer–Peppas release rate coefficient and in vivo absorption rate obtained with monocompartmental analysis of pharmacokinetic profile; (b) in vitro parameters (obtained from in vitro release and ex vivo permeation studies) and  $t_{max}MCA$ , for the 4 nasal powder formulations; (c) in vitro parameters and  $C_{max}$  for 3 nasal powder formulations, namely SDM of HPMC, SDM of PVP/VA and blend of HPMC and c) in vitro param-

eters and  $AUC_{1h}$  for the same 3 nasal powder formulations.  $AUC_{1h}$ , Area under the concentration time-curve from time zero to 1 h;  $C_{max}$ , Maximum peak concentration; HPMC - hydroxypropyl methylcellulose; IVR, in vitro release; PVP/VA - polyvinylpyrrolidone/vinyl acetate; SDM – spray-dried microparticles;  $t_{max}$ , time to achieve the maximum peak concentration;  $t_{max}MCA$ , time to achieve the maximum peak concentration using monocompartmental analysis

**Table 8** Pharmacokinetic parameters following intranasal administration of piroxicam nasal powders applying monocompartmental analysis

| Pharmacokinetic parameters <sup>a</sup> | SDM PVPVA | SDM HPMC | CA HPMC | Blend HPMC |
|-----------------------------------------|-----------|----------|---------|------------|
| $t_{max}MCA$ (h)                        | 1.60      | 0.44     | 1.11    | 1.75       |
| $k_a$ ( $h^{-1}$ )                      | 2.38      | 22.78    | 4.20    | 2.04       |
| $R^2$                                   | 0.9921    | 0.9851   | 0.9804  | 0.9834     |

<sup>a</sup> Parameters estimated considering a normalized PXC dose of 0.3 mg

CA – chimeral agglomerates; HPMC - hydroxypropyl methylcellulose;  $k_a$ , in vivo absorption rate; PVP/VA - polyvinylpyrrolidone/vinyl acetate; SDM – spray-dried microparticles;  $t_{max}MCA$ , time to achieve the maximum peak concentration using monocompartmental analysis

in the literature for PXC pharmacokinetic analysis (Gwak et al. 2005). The model provided good fits ( $R^2 > 0.98$ ) and allowed better discrimination of formulations in  $t_{max}$  (Table 8).

The coefficients of determination ( $R^2$ ) of the linear correlations between the aforementioned parameters are presented in Table 9. The results showed that in vitro parameters better correlate with  $t_{max}MCA$  (Fig. 6b), with the highest correlation between  $t_{max}MCA$  and ex vivo permeation at 0.33 h ( $R^2 = 0.9781$ ). As previously mentioned, the fast drug release and permeation in early timepoints affected drug absorption decreasing  $t_{max}$ . Aiming at a fast onset of action for a poorly soluble drug, amorphous nasal formulations with high release rate could then be an adequate formulation strategy.

**Table 9** Matrix with the coefficients of determination ( $R^2$ ) of the linear correlations between in vitro and in vivo parameters, for the 4 nasal powder formulations

| $R^2$                        | $C_{\max}$ | $t_{\max}$ | $t_{\max}$ MCA | $AUC_{1h}$ |
|------------------------------|------------|------------|----------------|------------|
| Ex vivo permeation at 1 h    | 0.4061     | 0.6589     | 0.9383         | 0.6286     |
| Ex vivo permeation at 0.33 h | 0.6473     | 0.9063     | 0.9781         | 0.8834     |
| IVR at 1 h                   | 0.3466     | 0.8158     | 0.9736         | 0.6406     |
| IVR at 0.33 h                | 0.3772     | 0.8565     | 0.9773         | 0.6772     |

$AUC_{1h}$ , Area under the concentration time-curve from time zero to 1 h;  $C_{\max}$ , Maximum peak concentration; IVR, in vitro release;  $t_{\max}$ , time to achieve the maximum peak concentration;  $t_{\max}$  MCA, time to achieve the maximum peak concentration using monocompartmental analysis

**Table 10** Matrix with the coefficients of determination ( $R^2$ ) of the linear correlations between in vitro and in vivo parameters, for 3 nasal powder formulations namely SDM of HPMC, SDM of PVP/VA and blend of HPMC.

| $R^2$                        | $C_{\max}$ | $t_{\max}$ | $t_{\max}$ MCA | $AUC_{1h}$ |
|------------------------------|------------|------------|----------------|------------|
| Ex vivo permeation at 1 h    | 0.9614     | 0.7179     | 0.9425         | 0.8899     |
| Ex vivo permeation at 0.33 h | 0.9969     | 0.9089     | 0.9999         | 0.9928     |
| IVR at 1 h                   | 0.9906     | 0.9314     | 0.9972         | 0.9981     |
| IVR at 0.33 h                | 0.9802     | 0.9519     | 0.9907         | 1.0000     |

$AUC_{1h}$ , Area under the concentration time-curve from time zero to 1 h;  $C_{\max}$ , Maximum peak concentration; HPMC - hydroxypropyl methylcellulose; IVR, in vitro release; PVP/VA - polyvinylpyrrolidone/vinyl acetate; SDM – spray-dried microparticles;  $t_{\max}$ , time to achieve the maximum peak concentration;  $t_{\max}$  MCA, time to achieve the maximum peak concentration using monocompartmental analysis

As mentioned in Sect. 3.5., chimeral agglomerates of HPMC showed an unexpected pharmacokinetic profile, with low  $C_{\max}$  and  $AUC_t$ , possibly due to partial drug deglutition or lung delivery. Therefore, additional correlations were performed with the remaining three formulations. Without chimeral agglomerates of HPMC,  $R^2$  increased for all parameters (Table 10). In addition to  $t_{\max}$  MCA, correlation between in vitro parameters and  $C_{\max}$  or  $AUC_{1h}$  showed a  $R^2$  of 0.9969 for the correlation between ex vivo permeation at 0.33 h and  $C_{\max}$  and a  $R^2$  of 1.0000 for the correlation between in vitro release at 0.33 h and  $AUC_{1h}$  (Fig. 6c-d). An inherent limitation of removing one of the formulations is the reduction of the degrees of freedom in the linear regression model, which reduces the precision of the estimates and the power of the model.

Overall, correlations with ex vivo permeation were stronger at the first timepoint of 0.33 h compared with the 1 h timepoint. This suggests that drug supersaturation, even when maintained for a short period of time, affects absorption.

In general, in vitro release and ex vivo permeation studies with vertical Franz diffusion cells showed strong

correlations with  $C_{\max}$ ,  $t_{\max}$  MCA and  $AUC_{1h}$  for three formulations, suggesting that these methods are biorelevant and provide valuable insights into drug nasal absorption. Furthermore, the in vitro drug release method is simple and easier to implement in the industry than methods that require excised tissues as ex vivo permeation studies. Therefore, for formulations without permeability modifiers, in vitro drug release testing could be preferred over ex vivo permeation studies. In vitro studies were conducted over 8 h, providing information on the drug release and permeation over a longer time frame. However, a shorter time frame of 2 h could have been sufficient for formulation development and ranking. This time frame is consistent with the rapid drug dissolution and absorption that occurs at the nasal mucosa that is time-limited by the mucociliary clearance, which is responsible for the renewal of nasal mucus every 15 to 20 min (Martín et al. 1998). The results suggest that in vitro drug release studies are a suitable performance methodology to guide early stages of nasal powder formulation development, being useful for the estimation of the absorption behavior of nasal powders including ASD formulations and the selection of the most promising prototypes to move forward to in vivo studies.

## Conclusion

The present work aimed to evaluate the performance of different powders for nasal delivery of a poorly soluble drug, including ASD formulations, and evaluate the in vivo predictability of in vitro/ex vivo models. To the best of our knowledge, this is the first report on correlations between in vitro and in vivo performance of nasal powder formulations manufactured by three manufacturing strategies, including ASDs.

HPMC-based amorphous formulations showed enhanced drug release and permeation across porcine mucosa, compared to PVP/VA formulations and blends. This polymer may sustain the supersaturated drug for a longer period of time, compared with PVP/VA. Nasal deposition of HPMC chimeral agglomerates was higher in NGI stages, suggesting off-target deposition.

In vivo pharmacokinetic studies revealed fast drug absorption from nasal powders, especially from ASDs, with correlations between the release and absorption rates and between in vitro performance and  $t_{\max}$ . This indicates that ASDs for nasal delivery of poorly soluble drugs could be a suitable strategy to provide a faster onset of action, which could be valuable for several therapeutic indications, such as pain management, migraine or angina pectoris (Fortuna et al. 2014).  $C_{\max}$  and  $AUC_{1h}$  also revealed good correlation with in vitro release and ex vivo permeation studies in

early timepoints where absorption largely occurs, but only for formulations with more nasal targeted deposition.

Regulatory guidelines are focused on extended release oral dosage forms (Food and Drug Administration 1997; European Medicines Agency 2014). For non-oral drug products, as nasal powders, IVIVC can be more challenging due to lack of standardized in vitro methods and nasal delivery complexity (Henriques et al. 2022). However, establishing IVIVC for these products should support the use of in vitro methods, guide formulation development and ensure product quality (Shen and Burgess 2015). In the present work, successful IVIVC were established between in vivo absorption rate and in vitro drug release rates as well as between in vivo pharmacokinetic parameters ( $t_{max}$ ,  $C_{max}$  and  $AUC_{1h}$ ) and in vitro drug release and ex vivo drug permeation at early timepoints. This supports the use of Franz diffusion cells to study drug release and permeation of nasal powder formulations. The in vitro/ex vivo performance methods used proved to be biorelevant and provided valuable insights into drug nasal absorption. For poorly soluble drugs without permeability challenges, ex vivo permeation studies may not add value to in vitro release testing, considering the similar profiles obtained. Additionally, nasal deposition also plays a major role on absorption. Therefore, deposition studies should be conducted in parallel.

For orally inhaled drug products, predictive in vitro methodologies comprise a prior aerosolization of the powder and collection of representative particles that would deposit on the lung, before physiologically relevant in vitro dissolution (Radivojev et al. 2019). For nasal powders, future work includes the development of integrated particle deposition and dissolution/drug release methodologies that would provide better predictability and phenomena understanding in nasal powder formulation development.

**Supplementary Information** The online version contains supplementary material available at <https://doi.org/10.1007/s40005-023-00630-1>.

**Acknowledgments** This research was funded by FCT (Fundação para a Ciência e Tecnologia), Portugal under the doctor fellowship 2021.06125.BD, and by FCT and Hovione under the doctoral fellowship PD/BDE/150298/2019.

**Funding** Open access funding provided by FCT|FCCN (b-on).

## Declarations

**Statement of Human and Animal Rights** All animal procedures were conducted in agreement with the international regulations of the European Directive (2010/63/EU) regarding the protection of laboratory animals used for scientific purposes and with the Portuguese law on animal welfare (Decree-Law 113/2013). The experimental and care procedures were reviewed and approved by the Animal Welfare Board (ORBEA, 02-2021—Órgão Responsável pelo Bem-Estar Animal) at the Faculty of Pharmacy of the University of Coimbra and the Por-

tuguese Directorate-General for Food and Veterinary (DGAV). This article does not contain any studies with human participants performed by any of the authors.

**Conflict of interest** All authors (P. Henriques, J. Bicker, A. Carona, M. Miranda, C. Vitorino, S. Doktorovová, and A. Fortuna) declare that they have no conflict of interest.

**Open Access** This article is licensed under a Creative Commons Attribution 4.0 International License, which permits use, sharing, adaptation, distribution and reproduction in any medium or format, as long as you give appropriate credit to the original author(s) and the source, provide a link to the Creative Commons licence, and indicate if changes were made. The images or other third party material in this article are included in the article's Creative Commons licence, unless indicated otherwise in a credit line to the material. If material is not included in the article's Creative Commons licence and your intended use is not permitted by statutory regulation or exceeds the permitted use, you will need to obtain permission directly from the copyright holder. To view a copy of this licence, visit <http://creativecommons.org/licenses/by/4.0/>.

## References

- Amidon GL, Lennernäs H, Shah VP, Crison JR (1995) A theoretical basis for a Biopharmaceutic Drug classification: the correlation of in Vitro Drug Product Dissolution and in vivo bioavailability. *Pharm Res* 12:413–420. <https://doi.org/10.1023/A:1016212804288/METRICS>
- Balducci AG, Ferraro L, Bortolotti F et al (2013) Antidiuretic effect of desmopressin chimera agglomerates by nasal administration in rats. *Int J Pharm* 440:154–160. <https://doi.org/10.1016/J.IJPHARM.2012.09.049>
- Bao Q, Newman B, Wang Y et al (2018) In vitro and ex vivo correlation of drug release from ophthalmic ointments. *J Controlled Release* 276:93–101. <https://doi.org/10.1016/J.JCONREL.2018.03.003>
- Bartos C, Ambrus R, Sipos P et al (2015) Study of sodium hyaluronate-based intranasal formulations containing micro- or nano-sized meloxicam particles. *Int J Pharm* 491:198–207. <https://doi.org/10.1016/J.IJPHARM.2015.06.046>
- Bennett-Lenane H, O'Shea JP, O'Driscoll CM, Griffin BT (2020) A retrospective Biopharmaceutical analysis of > 800 approved oral drug products: are Drug Properties of Solid Dispersions and lipid-based formulations distinctive? *J Pharm Sci* 109:3248–3261. <https://doi.org/10.1016/j.xphs.2020.08.008>
- Bruschi ML (2015) Mathematical models of drug release. Strategies to modify the drug release from Pharmaceutical Systems. Elsevier, pp 63–86
- Buttini F, Colombo P, Rossi A et al (2012) Particles and powders: tools of innovation for non-invasive drug administration. *J Controlled Release* 161:693–702. <https://doi.org/10.1016/J.JCONREL.2012.02.028>
- Chen JZ, Kiaee M, Martin AR, Finlay WH (2020) In vitro assessment of an idealized nose for nasal spray testing: comparison with regional deposition in realistic nasal replicas. *Int J Pharm* 582:119341. <https://doi.org/10.1016/J.IJPHARM.2020.119341>
- Chen JZ, Finlay WH, Martin A (2022) In Vitro Regional Deposition of Nasal Sprays in an Idealized Nasal Inlet: comparison with in vivo Gamma Scintigraphy. *Pharm Res* 39:3021–3028. <https://doi.org/10.1007/S11095-022-03388-7>
- Cho W, Kim M-S, Jung M-S et al (2015) Design of salmon calcitonin particles for nasal delivery using spray-drying and novel

- supercritical fluid-assisted spray-drying processes. *Int J Pharm* 478:288–296. <https://doi.org/10.1016/J.IJPHARM.2014.11.051>
- Colombo P, Santi P, Bettini R et al (2005) Powder for nasal administration of drugs
- Colombo G, Bortolotti F, Chiapponi V et al (2016) Nasal powders of thalidomide for local treatment of nose bleeding in persons affected by hereditary hemorrhagic telangiectasia. *Int J Pharm* 514:229–237. <https://doi.org/10.1016/J.IJPHARM.2016.07.002>
- Cunha S, Swedrowska M, Bellahmid Y et al (2022) Thermosensitive in situ hydrogels of rivastigmine-loaded lipid-based nanosystems for nose-to-brain delivery: characterisation, biocompatibility, and drug deposition studies. *Int J Pharm* 620:121720. <https://doi.org/10.1016/J.IJPHARM.2022.121720>
- D'Angelo D, Kooij S, Verhoeven F et al (2023) Fluorescence-enabled evaluation of nasal tract deposition and coverage of pharmaceutical formulations in a silicone nasal cast using an innovative spray device. *J Adv Res* 44:227–232. <https://doi.org/10.1016/j.jare.2022.04.011>
- Dalpiaz A, Gavini E, Colombo G et al (2008) Brain uptake of an anti-ischemic agent by nasal administration of microparticles. *J Pharm Sci* 97:4889–4903. <https://doi.org/10.1002/JPS.21335>
- Dalpiaz A, Fogagnolo M, Ferraro L et al (2015) Nasal chitosan microparticles target a zidovudine prodrug to brain HIV sanctuaries. *Antiviral Res* 123:146–157. <https://doi.org/10.1016/J.ANTIVIRAL.2015.09.013>
- de Souza Lima R, Ré MI, Arlabosse P (2020) Drying droplet as a template for solid formation: a review. *Powder Technol* 359:161–171. <https://doi.org/10.1016/j.powtec.2019.09.052>
- Elmowafy E, Osman R, El-Shamy AEA, Awad GAS (2014) Nasal polysaccharides-glucose regulator microparticles: optimization, tolerability and antidiabetic activity in rats. *Carbohydr Polym* 108:257–265. <https://doi.org/10.1016/J.CARBPOL.2014.02.064>
- European Medicines Agency (2011) Guideline on bioanalytical method validation. <https://www.ema.europa.eu/en/bioanalytical-method-validation-scientific-guideline>. Accessed 24 Jun 2019
- European Medicines Agency (2014) Guideline on quality of oral modified release products. <https://www.ema.europa.eu/en/quality-oral-modified-release-products-scientific-guidelines>. Accessed 7 Mar 2023
- Farinha S, Sá JV, Lino PR et al (2022) Spray freeze drying of Biologics: a review and applications for Inhalation Delivery. *Pharm Res* 1:1–26. <https://doi.org/10.1007/S11095-022-03442-4>
- Food and Drug Administration (1989) FDA-Approved Drugs - Sprix. In: New Drug Application (NDA): 022382. <https://www.accessdata.fda.gov/scripts/cder/daf/index.cfm?event=BasicSearch.process>. Accessed 26 Apr 2023
- Food and Drug Administration (1997) Guidance for Industry - Extended Release Oral Dosage Forms: Development, Evaluation, and Application of In Vitro/In Vivo Correlations. <https://www.fda.gov/media/70939/download>. Accessed 24 Jun 2019
- Food and Drug Administration (2018) Bioanalytical Method Validation Guidance for Industry. <https://www.fda.gov/media/70858/download>. Accessed 24 Jun 2019
- Food and Drug Administration (2023) Inactive Ingredients for Approved Drug Products. <https://www.accessdata.fda.gov/scripts/cder/iig/index.cfm?event=BasicSearch.page>. Accessed 8 May 2023
- Fortuna A, Alves G, Serralheiro A et al (2014) Intranasal delivery of systemic-acting drugs: small-molecules and biomacromolecules. *Eur J Pharm Biopharm* 88:8–27. <https://doi.org/10.1016/J.EJPB.2014.03.004>
- Fransén N, Espefält Westin U, Nyström C, Björk E (2007) The in vitro transport of dihydroergotamine across porcine nasal respiratory and olfactory mucosa and the effect of a novel powder formulation. *J Drug Deliv Sci Technol* 17:267–271. [https://doi.org/10.1016/S1773-2247\(07\)50094-8](https://doi.org/10.1016/S1773-2247(07)50094-8)
- Furubayashi T, Inoue D, Nishiyama N et al (2020) Comparison of various cell lines and three-dimensional mucociliary tissue model systems to estimate drug permeability using an in vitro transport study to predict nasal drug absorption in rats. *Pharmaceutics* 12:79. <https://doi.org/10.3390/pharmaceutics12010079>
- Gavini E, Hegge AB, Rasso G et al (2006) Nasal administration of carbamazepine using chitosan microspheres: in vitro/in vivo studies. *Int J Pharm* 307:9–15. <https://doi.org/10.1016/J.IJPHARM.2005.09.013>
- Gavini E, Rasso G, Ferraro L et al (2011) Influence of Chitosan Glutamate on the in vivo intranasal absorption of Rokitamycin from Microspheres. *J Pharm Sci* 100:1488–1502. <https://doi.org/10.1002/JPS.22382>
- Gieszinger P, Kiss T, Szabó-Révész P, Ambrus R (2021) The development of an in vitro horizontal diffusion cell to monitor nasal powder penetration inline. *Pharmaceutics* 13:809. <https://doi.org/10.3390/PHARMACEUTICS13060809>
- Gomes dos Reis L, Ghadiri M, Young P, Traini D (2020) Nasal powder formulation of Tranexamic Acid and Hyaluronic Acid for the treatment of Epistaxis. *Pharm Res* 37:1–14. <https://doi.org/10.1007/s11095-020-02913-w>
- Gonçalves VSS, Matias AA, Póejo J et al (2016) Application of RPMI 2650 as a cell model to evaluate solid formulations for intranasal delivery of drugs. *Int J Pharm* 515:1–10. <https://doi.org/10.1016/J.IJPHARM.2016.09.086>
- Gonçalves D, Alves G, Fortuna A et al (2017) Pharmacokinetics of opicapone, a third-generation COMT inhibitor, after single and multiple oral administration: a comparative study in the rat. *Toxicol Appl Pharmacol* 323:9–15. <https://doi.org/10.1016/j.taap.2017.03.013>
- Gonçalves J, Silva S, Gouveia F et al (2021) A combo-strategy to improve brain delivery of antiepileptic drugs: Focus on BCRP and intranasal administration. *Int J Pharm* 593:120161. <https://doi.org/10.1016/j.ijpharm.2020.120161>
- Gwak HS, Choi JS, Choi HK (2005) Enhanced bioavailability of piroxicam via salt formation with ethanolamines. *Int J Pharm* 297:156–161. <https://doi.org/10.1016/J.IJPHARM.2005.03.016>
- Hasçıçek C, Gönül N, Erk N (2003) Mucoadhesive microspheres containing gentamicin sulfate for nasal administration: preparation and in vitro characterization. *Il Farmaco* 58:11–16. [https://doi.org/10.1016/S0014-827X\(02\)00004-6](https://doi.org/10.1016/S0014-827X(02)00004-6)
- Henriques P, Marques J, Paisana M et al (2021) Benchmarking of particle engineering technologies for nasal powder manufacture. *J Aerosol Med Pulm Drug Deliv* 34:A7. <https://ddl-conference.com/ddl2020-christmas-lectures/conference-papers/benchmarking-of-particle-engineering-technologies-for-nasal-powder-manufacture/>
- Henriques P, Fortuna A, Doktorovová S (2022) Spray dried powders for nasal delivery: process and formulation considerations. *Eur J Pharm Biopharm* 176:1–20. <https://doi.org/10.1016/J.EJPB.2022.05.002>
- Henriques P, Bicker J, Silva S, Doktorovová S, Fortuna A (2023 August) Nasal-PAMPA: a novel non-cell-based high throughput screening assay for prediction of nasal drug permeability. *Int J Pharm* 643:123252. <https://doi.org/10.1016/j.ijpharm.2023.123252>
- Horváth T, Ambrus R, Völgyi G et al (2016) Effect of solubility enhancement on nasal absorption of meloxicam. *Eur J Pharm Sci* 95:96–102. <https://doi.org/10.1016/j.ejps.2016.05.031>
- Huh Y, Cho H-J, Yoon I-S et al (2010) Preparation and evaluation of spray-dried hyaluronic acid microspheres for intranasal delivery of fexofenadine hydrochloride. *Eur J Pharm Sci* 40:9–15. <https://doi.org/10.1016/J.EJPS.2010.02.002>
- International Council For Harmonisation of Technical Requirements for Pharmaceuticals for Human Use (2022) ICH guideline M10 on bioanalytical method validation and study sample analysis.

- <https://www.ich.org/page/multidisciplinary-guidelines>. Accessed 1 Mar 2023
- Jug M, Bećirević-Lačan M (2008) Development of a cyclodextrin-based nasal delivery system for Lorazepam. *Drug Dev Ind Pharm* 34:817–826. <https://doi.org/10.1080/03639040801926063>
- Jug M, Hafner A, Lovrić J et al (2018) An overview of in vitro dissolution/release methods for novel mucosal drug delivery systems. *J Pharm Biomed Anal* 147:350–366. <https://doi.org/10.1016/J.JPBA.2017.06.072>
- Jüptner A, Sarrailh S, Scherließ R (2019) Spray dried powders for nasal application - influence of particle morphology and filling process on aerosol generation. *J Aerosol Med Pulm Drug Deliv* 32:A4–A4
- Jüptner A, Scherließ R (2020) Spray dried formulations for inhalation—meaningful characterisation of powder properties. *Pharmaceutics* 12:14. <https://doi.org/10.3390/pharmaceutics12010014>
- Jurišić Dukovski B, Mrak L, Winnicka K et al (2019) Spray-dried nanoparticle-loaded pectin microspheres for dexamethasone nasal delivery. *Drying Technol* 37:1915–1925. <https://doi.org/10.1080/07373937.2018.1545783>
- Karavasili C, Bouropoulos N, Sygellou L et al (2016) PLGA/DPPC/trimethylchitosan spray-dried microparticles for the nasal delivery of ropinirole hydrochloride: in vitro, ex vivo and cytocompatibility assessment. *Mater Sci Engineering: C* 59:1053–1062. <https://doi.org/10.1016/J.MSEC.2015.11.028>
- Kiaee M, Wachtel H, Noga ML et al (2019) An idealized geometry that mimics average nasal spray deposition in adults: a computational study. *Comput Biol Med* 107:206–217. <https://doi.org/10.1016/j.compbimed.2019.02.013>
- Kundoor V, Dalby RN (2011) Effect of formulation- and administration-related variables on deposition pattern of nasal spray pumps evaluated using a nasal cast. *Pharm Res* 28:1895–1904. <https://doi.org/10.1007/S11095-011-0417-6/FIGURES/13>
- Marple VA, Olson BA, Santhanakrishnan K et al (2004) Next generation pharmaceutical impactor: a new impactor for pharmaceutical inhaler testing. Part III. Extension of archival calibration to 15 L/min. *J Aerosol Med* 17:335–343. <https://doi.org/10.1089/JAM.2004.17.335>
- Martind E, Schipper NGM, Verhoef JC, Merkus FWHM (1998) Nasal mucociliary clearance as a factor in nasal drug delivery. *Adv Drug Deliv Rev* 29:13–38. [https://doi.org/10.1016/S0169-409X\(97\)00059-8](https://doi.org/10.1016/S0169-409X(97)00059-8)
- Mirza S, Miroshnyk I, Habib MJ et al (2010) Enhanced dissolution and oral bioavailability of Piroxicam Formulations: modulating effect of phospholipids. *Pharmaceutics* 2:339. <https://doi.org/10.3390/PHARMACEUTICS2040339>
- Murphy B, Aisenstat M, Ordoubadi M et al (2022) Intranasal Powder Administration of a spray-dried tuberculosis vaccine candidate characterized using the Alberta Idealized Nasal Inlet. *Respiratory Drug Delivery* 1:441–446
- Mygind N, Dahl R (1998) Anatomy, physiology and function of the nasal cavities in health and disease. *Adv Drug Deliv Rev* 29:3–12. [https://doi.org/10.1016/S0169-409X\(97\)00058-6](https://doi.org/10.1016/S0169-409X(97)00058-6)
- Newman A (2015) *Pharmaceutical amorphous solid dispersions*. John Wiley & Sons, Hoboken, New Jersey
- Nunes PD, Pinto JF, Henriques J, Paiva AM (2022) Insights into the release mechanisms of ITZ:HPMCAS Amorphous Solid Dispersions: the Role of Drug-Rich Colloids. *Mol Pharm* 19:51–66. <https://doi.org/10.1021/acs.molpharmaceut.1c00578>
- Nunes PD, Ferreira AF, Pinto JF et al (2023) In vitro Dissolution/Permeation tools for amorphous solid dispersions bioavailability forecasting II: comparison and mechanistic insights. *Eur J Pharm Sci* 106513. <https://doi.org/10.1016/j.ejps.2023.106513>
- Papakyriakopoulou P, Manta K, Kostantini C et al (2021) Nasal powders of quercetin- $\beta$ -cyclodextrin derivatives complexes with mannitol/lecithin microparticles for nose-to-brain delivery: in vitro and ex vivo evaluation. *Int J Pharm* 607:121016. <https://doi.org/10.1016/J.IJPB.2021.121016>
- Phillips DJ, Pygall SR, Cooper VB, Mann JC (2012) Overcoming sink limitations in dissolution testing: a review of traditional methods and the potential utility of biphasic systems. *J Pharm Pharmacol* 64:1549–1559. <https://doi.org/10.1111/J.2042-7158.2012.01523.X>
- Pozzoli M, Traini D, Young PM et al (2017) Development of a Soluplus budesonide freeze-dried powder for nasal drug delivery. *Drug Dev Ind Pharm* 43:1510–1518. <https://doi.org/10.1080/03639045.2017.1321659>
- Radivojev S, Zellnitz S, Paudel A, Fröhlich E (2019) Searching for physiologically relevant in vitro dissolution techniques for orally inhaled drugs. *Int J Pharm* 556:45–56. <https://doi.org/10.1016/J.IJPB.2018.11.072>
- Rasetti-Escargueil C, Grangé V (2005) Pharmacokinetic profiles of two tablet formulations of piroxicam. *Int J Pharm* 295:129–134. <https://doi.org/10.1016/J.IJPB.2005.02.006>
- Rassu G, Soddu E, Cossu M et al (2015) Solid microparticles based on chitosan or methyl- $\beta$ -cyclodextrin: a first formulative approach to increase the nose-to-brain transport of deferoxamine mesylate. *J Controlled Release* 201:68–77. <https://doi.org/10.1016/J.JCONREL.2015.01.025>
- Rassu G, Ferraro L, Pavan B et al (2018) The role of combined penetration enhancers in nasal microspheres on in vivo drug bioavailability. *Pharmaceutics* 10:206. <https://doi.org/10.3390/pharmaceutics10040206>
- Russo P, Buttini F, Sonvico F et al (2004) Chimeral agglomerates of microparticles for the administration of caffeine nasal powders. *J Drug Deliv Sci Technol* 14:449–454. [https://doi.org/10.1016/S1773-2247\(04\)50083-7](https://doi.org/10.1016/S1773-2247(04)50083-7)
- Salamat-Miller N, Chittchang M, Johnston TP (2005) The use of mucoadhesive polymers in buccal drug delivery. *Adv Drug Deliv Rev* 57:1666–1691
- Serralheiro A, Alves G, Fortuna A, Falcão A (2014) Intranasal administration of carbamazepine to mice: a direct delivery pathway for brain targeting. *Eur J Pharm Sci* 60:32–39. <https://doi.org/10.1016/J.EJPS.2014.04.019>
- Shen J, Burgess DJ (2015) In vitro-in vivo correlation for complex non-oral drug products: where do we stand? *J Controlled Release* 219:644–651. <https://doi.org/10.1016/j.jconrel.2015.09.052>
- Simões A, Veiga F, Vitorino C (2020) Progressing towards the sustainable development of cream formulations. *Pharmaceutics* 12:647. <https://doi.org/10.3390/pharmaceutics12070647>
- Sosnik A, Das Neves J, Sarmento B (2014) Mucoadhesive polymers in the design of nano-drug delivery systems for administration by non-parenteral routes: a review. *Prog Polym Sci* 39:2030–2075
- Suwabe S, Tagami T, Ogawa K, Ozeki T (2023) Improved drug transfer into brain tissue via the nose-to-brain approach using suspension or powder formulations based on the amorphous solid dispersion technique. *Eur J Pharm Biopharm* 185:137–147. <https://doi.org/10.1016/j.ejpb.2023.02.012>
- Szabó-Révész P (2018) Modifying the physicochemical properties of NSAIDs for nasal and pulmonary administration. *Drug Discov Today Technol* 27:87–93. <https://doi.org/10.1016/J.DDTEC.2018.03.002>
- Tas C, Ozkan CK, Savaser A et al (2009) Nasal administration of metoclopramide from different dosage forms: in vitro, ex vivo, and in vivo evaluation. *Drug Deliv* 16:167–175. <https://doi.org/10.1080/10717540902764172>
- Tiozzo Fasiolo L, Manniello MD, Tratta E et al (2018) Opportunity and challenges of nasal powders: drug formulation and delivery. *Eur J Pharm Sci* 113:2–17. <https://doi.org/10.1016/J.EJPS.2017.09.027>
- Tiozzo Fasiolo L, Manniello MD, Bortolotti F et al (2019) Anti-inflammatory flurbiprofen nasal powders for nose-to-brain delivery in

- Alzheimer's disease. *J Drug Target* 27:984–994. <https://doi.org/10.1080/1061186X.2019.1574300>
- Tiozzo Fasiolo L, Dario Manniello M, Banella S et al (2021) Flurbiprofen Sodium Microparticles and Soft Pellets for nose-to-brain delivery: serum and brain levels in rats after nasal insufflation. *Int J Pharm* 605:120827. <https://doi.org/10.1016/j.ijpharm.2021.120827>
- Trenkel M, Scherließ R (2021) Nasal powder formulations: In-Vitro Characterisation of the impact of powders on nasal Residence Time and sensory Effects. *Pharmaceutics* 13:385. <https://doi.org/10.3390/PHARMACEUTICS13030385>
- Trenkel M, Scherließ R (2023) Optimising nasal powder drug delivery – characterisation of the effect of excipients on drug absorption. *Int J Pharm* 633:122630. <https://doi.org/10.1016/J.IJPHARM.2023.122630>
- Trows S, Scherließ R (2016) Carrier-based dry powder formulation for nasal delivery of vaccines utilizing BSA as model drug. *Powder Technol* 292:223–231. <https://doi.org/10.1016/J.POWTEC.2016.01.042>
- Ugwoke MI, Agu RU, Verbeke N, Kinget R (2005) Nasal mucoadhesive drug delivery: background, applications, trends and future perspectives. *Adv Drug Deliv Rev* 57:1640–1665. <https://doi.org/10.1016/J.ADDR.2005.07.009>
- USP-NF 601 Inhalation and Nasal Drug Products: Aerosols, Sprays, and Powders—Performance Quality Tests. In: United States Pharmacopeia 43-NF38 2S
- Van Eerdenbrugh B, Baird JA, Taylor LS (2010) Crystallization tendency of active pharmaceutical ingredients following rapid solvent evaporation - classification and comparison with crystallization tendency from undercooled melts. *J Pharm Sci* 99:3826–3838. <https://doi.org/10.1002/jps.22214>
- Vig B, Morgen M (2017) Formulation, process development, and Scale-Up: spray-drying amorphous solid dispersions for insoluble drugs. *Developing solid oral dosage forms*, 2nd edn. Academic Press, pp 793–820
- Vitorino C, Silva S, Gouveia F et al (2020) QbD-driven development of intranasal lipid nanoparticles for depression treatment. *Eur J Pharm Biopharm* 153:106–120. <https://doi.org/10.1016/j.ejpb.2020.04.011>
- Wadell C, Björk E, Camber O (1999) Nasal drug delivery—evaluation of an in vitro model using porcine nasal mucosa. *Eur J Pharm Sci* 7:197–206. [https://doi.org/10.1016/S0928-0987\(98\)00023-2](https://doi.org/10.1016/S0928-0987(98)00023-2)
- Wadell C, Björk E, Camber O (2003) Permeability of porcine nasal mucosa correlated with human nasal absorption. *Eur J Pharm Sci* 18:47–53. [https://doi.org/10.1016/S0928-0987\(02\)00240-3](https://doi.org/10.1016/S0928-0987(02)00240-3)
- Williams HD, Trevaskis NL, Charman SA et al (2013) Strategies to address low drug solubility in Discovery and Development. *Pharmacol Rev* 65:315–499. <https://doi.org/10.1124/PR.112.005660>

**Publisher's Note** Springer Nature remains neutral with regard to jurisdictional claims in published maps and institutional affiliations.